Response to Review on 'Air-borne in-situ measurements of aerosol size distributions and BC across the IGP during SWAAMI-RAWEX' by Mukunda Madhab Gogoi et al., (ACP-2020-144).

Response to Reviewer-1

This paper presents altitude profiles of aerosol size distribution and Black carbon obtained through in situ on-board research aircraft as a part of South-West Asian Aerosol Monsoon Interaction (SWAAMI) experiment conducted jointly under Indo-UK project over three distinct locations (Jodhpur, Varanasi, and Bhubaneswar) just prior to the onset of Indian Summer Monsoon. Simultaneous measurements from Cloud Aerosol Transportation System (CATS) on-board International Space Station and OMI measurements are also used as supporting information.

Major results include an increase in coarse mode concentration and coarse mode mass-fraction with increase in altitude across the entire IGP, especially above the well-mixed region. Further authors found increase with altitude in both the mode radii and geometric mean radii of the size distributions. Near the surface the features were specific to the different sub-regions ie., highest coarse mode mass fraction in the western IGP and highest accumulation fraction in the Central IGP with the eastern IGP coming in-between. The elevated coarse mode fraction is attributed to mineral dust load arising from local production as well as due to advection from the west which is further verified using CATS measurements. Existence of a well-mixed BC variation up to the ceiling altitude (3.5 km) is reiterated in this manuscript and match well with those obtained using previous aircraft and balloon platforms.

Results presented in the manuscript are in general unique and apt for the prestigious journal like ACP. Manuscript is written preciously and concise except at few places. The results present also add new understanding on the size distribution of aerosol concentration in both altitudinal and longitudinally which are very important in understanding their role on precipitation processes besides radiative forcing estimates. Though major part of manuscript is written well, at some place revision is required. Manuscript may be acceptable after satisfactory revising the following.

We appreciate the summary evaluation of the reviewer and agree to the observations. Following the valuable comments and fruitful suggestions for improving the quality of the manuscript, we have revised it incorporating the review comments of all the reviewers. Our point wise response to each of the comment is given below in bold letters, below the respective comments.

Major comments/suggestions:

It is not clear from where and how rainfall and relative humidity measurements presented in Figure 2e are obtained. Further they are not discussed at all in the rest of the manuscript. Same for the profiles of temperature presented in figure 2f.

I suggest providing profiles of temperature and relative humidity (if obtained from aircraft) as a separate figure in Supplementary material and add related discussion the manuscript. This information may be useful while dealing with hygroscopic nature of aerosol.

Response: The values of surface meteorological parameters were obtained from the meteorological observations at the respective airports during the period of flight operations. In addition, ambient temperatures at different altitude levels of the atmosphere were obtained from the aircraft sensor. However, we did not have dedicated meteorological sensors and data loggers aboard for continuous recording of ambient RH and T. Hence, we are unable to

show the profiles. In view of this, we have modified Fig-2 in the revised manuscript and kept the relevant meteorological information (as numerical values) in the appropriate places.

It is not clear what is the source of the data (TPP) presented in Figure 12a. Further (b) and (c) are inter-changed. Note that SO2 is presented in (c) and NO2 in (b).

Response: Thanks for the suggestion. We have included the source of data (https://www.ntpc.co.in/en/power-generation/coal-based-power-stations) used to geo-locate the coal based TPP distributed over the Indian region. The inadvertent error in the figure caption (Figure-13-R1) is also corrected in the revised manuscript.

Measurements of Black Carbon with Aethalometer: Though authors made correction to the data obtained from Aethalometer, it is not clear how they have taken care of it in the un-pressurized air craft?

Response: We have elaborated the discussion (as given below) on the estimation of true BC concentrations from the unpressurised operation of aethalometer in the aircraft in the revised manuscript.

Line nos. 189-204: "In the present study, BC mass concentrations were obtained at 1-minute interval by operating the aethalometer at 50% of the maximum attenuation and a standard mass flow rate of 2 LPM corresponding to standard temperature (T_O, 293 K) and pressure (P_O, 1013 hPa). As the unpressurised aircraft climbed higher, the instrument experienced ambient pressure (P) and temperature (T). In order to maintain the set mass flow, the pumping speed of the instrument was automatically increased (through internal program) to aspire more volume of air. However, the volume of air aspirated at ambient pressure and temperature requires to be corrected to standard atmospheric condition for the actual estimate of BC (Moorthy et al., 2004). Thus, the actual volume of air aspirated by the Aethalometer at different atmospheric level is,

$$V = V_o \frac{P_o T}{P T_o}$$

Thus, true BC mass concentration (M_{BC}) is

$$M_{BC} = M^*_{BC} \left[\frac{P_O T}{P T_O}\right]^{-1} \quad (1)$$

Here, M^*_{BC} is the instrument measured raw mass concentration of BC at ambient pressure and temperature."

It will be good to show heating rates due to BC profiles at these three different regions. Some discussion is needed on how the results presented in the manuscript are linked with the main objective of the SWAAMI experiment.

Response: We comply with suggestion with thanks and have included the heating rate profiles due to BC at all the three distinct regions of the IGP. The

methodology of deriving BC forcing and atmospheric heating rate due to BC is included in the revised manuscript as given below:

<u>Line nos. 469-504</u>: "To quantify the climatic implications of BC, the heating rate profiles of BC are examined based on the estimation of shortwave direct radiative forcing (DRF) due to BC alone. The DRF due to BC represents the difference between the DRF for aerosols with and without the BC component. The in-situ values of scattering (σ_{sca}) and absorption (σ_{abs}) coefficients measured on-board the aircraft were used to estimate spectral values of AOD (layer-integrated σ_{sca} + σ_{abs}), single scattering albedo (SSA) and asymmetry parameter (g) for each level, assuming a well-mixed layer of 200 m above and below the measurement altitude (details are available in Vaishya et al., 2018). The layer mean values of AOD, SSA and Legendre moments of the aerosol phase function (derived from Henyey–Greenstein approximation) are used as input in the Santa Barbara DISORT Atmospheric Radiative Transfer (SBDART, Ricchiazzi et al., 1998) model to estimate diurnally averaged DRF (net flux with and without aerosols) at the top (DRF_{TOA}) and bottom (DRF_{SUR}) of each of the layers. The atmospheric forcing (DRF_{ATM}) for each of the levels is then estimated as

$$DRF_{ATM} = DRF_{TOA} - DRF_{SUR}$$

In order to estimate the forcing due to BC alone, optical parameters for aerosols were deduced again. For this, values of σ_{abs} were segregated to the contributions by BC (σ_{BC}) and OC (σ_{OC}), where σ_{BC} were estimated following inverse wavelength dependence of BC (e.g., Vaishya et al., 2017). Based on this, a new set of AOD and SSA for BC-free atmosphere is calculated and fed into SBDART for estimating DRF_{ALL-BC} without the BC component. Thus, DRF due to BC is

$$DRF_{BC} = DRF_{ALL} - DRF_{ALL-BC}$$

Here, DRF_{ALL} represents forcing due to all the aerosol components, including BC. Change in AOD from total to BC-free atmosphere is not significant (< 2%), whereas SSA changes to a greater extent which actually participates in the DRF_{BC} estimation.

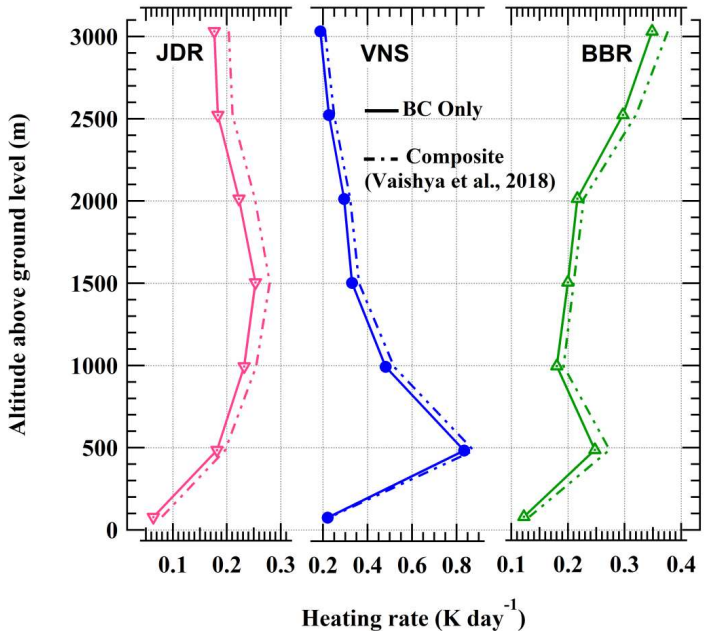

Figure-12: Vertical profiles of atmospheric heating rate due to BC (solid lines) and composite (dashed lines) aerosols for the regions of the IGP: (a) JDR in western IGP, (b) VNS in central IGP and (c) BBR in eastern IGP. Data for the composite heating rate profiles are from Vaishya et al., 2018.

The vertical profiles of atmospheric heating rate (HR, estimated based on the atmospheric pressure difference between top and bottom of each layer and aerosol induced forcing in that layer) due to BC alone shows (Figure-12) maximum influence of BC in trapping the SW-radiation at VNS, followed by BBR and JDR. Interestingly, the altitudinal profiles of heating rate are distinctly different over the regions, BBR showing an increase with altitude, while VNS shows the opposite pattern with maximum heating (~ (~ 0.81 K day^{-1}) near the surface. Enhanced heating at 500-2000 m altitude is seen at JDR. These results indicate the dominant role of absorbing aerosols near the surface at VNS, while the atmospheric perturbation due to elevated layers of absorbing aerosols is conspicuous at BBR (HR ~ 0.35 K day^{-1} at the ceiling altitude). The column integrated values of atmospheric forcing due to BC alone are 7.9 Wm^{-2}, 14.3 Wm^{-2} and 8.4 Wm^{-2} at JDR, VNS and BBR respectively."

Regarding the linkage of the results to the objectives of SWAAMI, we add (line nos. 78-88) the following.

"The information on aerosol size distribution is important for accurately describing the phase function, which describes the angular variation of the scattered intensity. The knowledge of its vertical variation would thus improve the accuracy of ARF estimation and hence heating rates. Such information is virtually non-existing over this region. Further, the knowledge of the variation of size distribution with altitude would be useful better understanding the aerosol-cloud interactions and CCN characteristics, during the evolving and active phase of the Indian monsoon. This was among the important information aimed to be obtained under SWAAMI - RAWEX (https://gtr.ukri.org/projects?ref=NE%2FL013886%2F1 and

http://www.spl.gov.in/SPL/index.php/arfs-research/field-campaigns/asfasf) - a joint Indo-UK field experiment involving airborne measurements using Indian and UK aircrafts during different phases of the Indian monsoon, right from just prior to the onset of monsoon (i.e. in the beginning of June).”

Minor issues:

Results presented in Page 4 at lines 90-94 and 111-121 are mostly repeating. Both can be clubbed and rewrite to the point.

Response: Complied with.

Figure 11 caption does not match with the information presented in the figure. I am unable to see (b) Daily profiles of MBC during each of the flight sorties on different days.

Response: Sorry for the oversight. We have corrected the figure caption in the revised manuscript.

Figure 14. Figure caption need to be changed as per the information presented in the Figure (It should be 18 and 20 May but not 19 and 20 May).

Response: Complied with.

I do not see any logic for presented vertical velocities for 2012, 2013 and 2016.

Response: We have shown the vertical velocities to support the role of changing dynamical processes during three distinct seasons (Winter, represented by December), Spring (represented by May) and just to prior to onset of Indian Summer Monsoon (represented by June), which very well support the vertical profiles of BC at the respective seasons. We have made this clear in the legends of the figure in the revised manuscript.

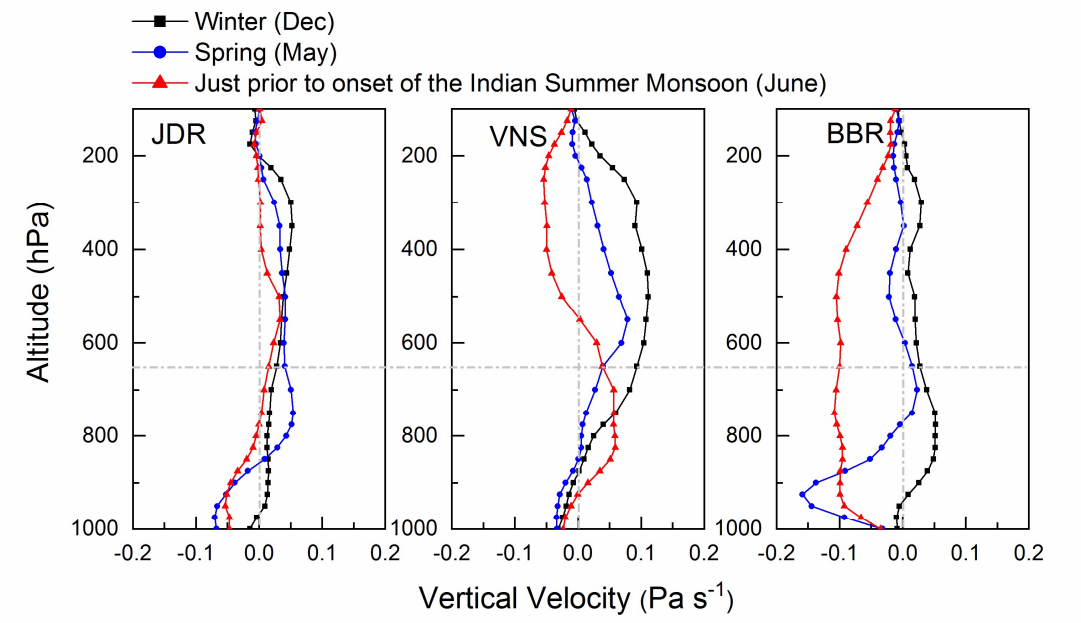

Figure-16: Vertical profiles of vertical velocity (Pa s^{-1}) over the study locations representing Winter (December, 2012), Spring (May, 2013) and just prior to the onset of the Indian Summer Monsoon (June, 2016) at different pressure levels from 1000 to 100 hPa. The positive and negative values are indicative of the descending and ascending motions respectively. The horizontal dashed line indicated the ceiling altitude (~ 3.5 km above ground level) of aircraft measurements while the vertical dashed lines mark the boundary of vertical velocity (= 0) changing from positive to negative and vice versa.

References:

Moorthy, K. K., Babu, S. S., Sunilkumar, S. V., Gupta, P. K., and Gera, B. S.: Altitude profiles of aerosol BC, derived from aircraft measurements over an inland urban location in India, Geophys. Res. Lett., 31, 1–4, https://doi.org/10.1029/2004GL021336, 2004.

Ricchiazzi, P., Yang, S., Gautier, C., and Sowle, D.: SBDART: A research and teaching software tool for plane-parallel radiative transfer in the Earth's atmosphere, B. Am. Meteor. Soc., 79,2101–2114, 1998.

Vaishya, A., Singh, P., Rastogi, S., and Babu, S. S.: Aerosol black carbon quantification in the central Indo-Gangetic Plain: Seasonal heterogeneity and source apportionment, Atmos. Res., 185,13–21, https://doi.org/10.1016/j.atmosres.2016.10.001, 2017.

Vaishya, A., Babu, S. N. S., Jayachandran, V., Gogoi, M. M., Lakshmi, N. B., Moorthy, K. K., and Satheesh, S. K.: Large contrast in the vertical distribution of aerosol optical properties and radiative effects across the Indo-Gangetic Plain during theSWAAMI–RAWEX campaign, Atmos. Chem. Phys., 18, 17669–17685, https://doi.org/10.5194/acp-18-17669-2018, 2018.

—END—

Response to Reviewer-2

The manuscript describes measurements of vertical profiles of size resolved number concentrations using an aerodynamic particle sizer and BC derived from a 7 channel aethalometer from three different going from west to east in the Indo Gangetic Plain (IGP). Measurements were made during an experiment named SWAAMI and the results from this experiment were discussed earlier in a couple of publications (Vaishya et al.,2018; and Govardhan et al.,2019) and probably others. There is a lack of vertical profile data of aerosols over the Indian sub-continent and in particular during the pre-monsoon season when the radiative balance over India and surrounding regions plays large role in driving the monsoon circulation. In that sense this paper is a welcome addition. However, the manuscript feels like the authors have tried to slice and dice the data in different ways but in the end doesn't seem to add anything new. It may be useful as a document of the data/analysis and I accept the paper with that view, though it often reads like a report than a research paper. The description of the dataset and the outcomes of the analysis is reasonable and there is not a lot that can be said in terms of any technical shortcomings of the arguments presented.

We thank the reviewer for the overall evaluation. We have addressed all the comments of the reviewer. Our response to each comment is shown by bold letters, below each comment.

Specific comments:

Line 462: The authors mention 'soot' emissions as of importance from thermal power plants. I generally assume this is primary fly ash and other suspended particulate matter (heavy metal containing particles). They seem to suggest there is soot and SPM and I am not sure what the distinction is?

Line 466: seems to suggest soot is BC. Are there any measurements in the power plant plumes to suggest that BC is a major emission from burning coal in power plants? I haven't come across this in discussions of power plant emissions elsewhere.

Response: Sorry for the lack of clarity. We agree with the reviewer that fly ash and SPM are major constituents in TPP emissions. Soot or BC is a major component in SPM. We have elaborated this in the revised manuscript, in addition to highlighting reported literature on BC measurements and characterization near coal burning power plants. The following has been added to the manuscript:

<u>Line nos. 505-522</u>: "In this context, we have examined the possible role of the large network of thermal power plants (TPP) over the northern part of India, which is reported to have significant contribution to regional emissions (Singh et al., 2018). These include the emissions of SO_2, NO_x, CO_2, CO, VOC, suspended particulate matter (PM2.5 and PM10, including BC and OC), and other trace metals like mercury (Guttikanda and Jawahar, 2014; Sahu et al., 2017) dispersing over large areas through stacks. Fly ash from coal-fired power plants causes severe environmental degradation in the nearby regions (5-10 km) of TPP (Tiwari et al., 2019). Over the IGP, since more than 70% of the thermal power plants are coal based, emissions of CO_2 and SO_2 hold more than 47% of the total emission share, while the relative share of PM2.5 and NOx are ~15% and 30% (GAINS, 2012). Based on in-situ measurement of BC, in fixed and transit areas, in close proximity of seven coal-fired TPP in Singrauli (located ~ 700 km north-west of BBR), Singh et al., (2018) have reported that BC concentration reached as high as 200 $\mu g.m^{-3}$ in the transit measurements.

The Energy and Resources Institute, India have also reported that emission levels of the carbonaceous (soot or BC) particles are estimated to be around 0.061 gm/kWh per unit of electricity from Indian thermal power plants (Vipradas et al., 2004). Based on emission pathways and ambient PM2.5 pollution over India, Venkataraman et al., (2018) have reported that the types of aerosols emitted from coal burning in thermal power plants and industry in eastern and peninsular India are similar to that of residential biomass combustion. These clearly indicate that TPP are major sources of BC in the atmosphere."

Figure 13: The figure shows the large fraction of the measurements with angstrom absorption exponents over values of 1 with median values of 1.3 and significant fraction near 1.5 and over. The authors say this is all fossil fuel emissions. Shouldn't these values of the angstrom absorption coefficient put these in the biomass burning and probably BrC range? Generally what fraction of the absorbing material measured using the technique used here fall in the BrC range as compared to BC?

Response: We are sorry for the lack of clarity on the discussion on Angstrom absorption exponent. We have taken care of the suggestion and revised the discussion on aerosol spectral absorption as given below:

<u>Line nos. 550-563</u>: "Based on laboratory studies and field investigations, it has already been shown that the higher values of α_{abs} (~ 2) are representative of BC from biomass burning emissions, while the values ~ 1 are indicative of BC from fossil fuel combustions (Kirchstetter et al., 2004). The values of α_{abs}> 1 are indicative of the presence of aerosols from biomass-burning, whose relative abundance increase with the steepness of the spectral absorption spectra, as has been reported elsewhere from the laboratory experiments [Hopkins et al., 2007].

Examining Figure 14 in the above light, it emerges that significant contribution of BC from fossil fuel combustions mixed with that from biomass burning origin prevails at higher altitudes over BBR, while the association between the two decreases abruptly from ML to higher heights at VNS. Consistently higher values of BC in the column associated with the values of α_{abs} lying between 1 and 1.5 can also be due to the ageing of BC at higher heights, during which BC mixes with other species and its Angstrom exponent increases, as the spectral dependence of absorption steepens when BC (even though its source could be fossil fuel) is coated with a concentric shell of weakly absorbing material (Gogoi et al., 2017). Further investigations are needed in this direction."

Figure 11: Either labels on the figure (namely figure (a) and figure(b)) or the title of the figure is either wrong or not clear

Response: Sorry for the oversight. We have corrected the Figure caption in the revised manuscript.

Figure 9: The focus of the figure is on values less than 0.3, the scale has just one color below that. It will be better if the color scale is recalibrated and plotted with the scale going from 0 to 0.5.

Response: Complied with. We have modified the figure in the revised manuscript as shown below.

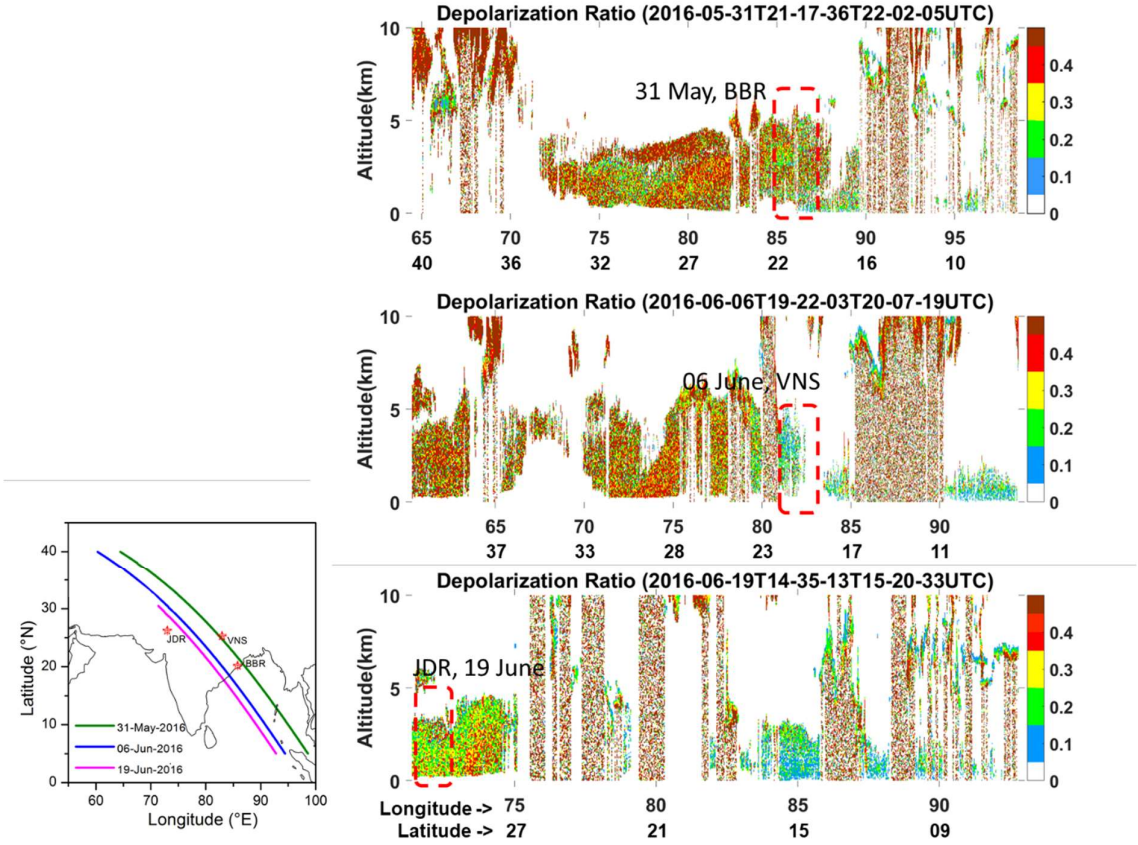

Line 290: The temperature in the western most location is said to be 40 C. This should make this location have the deepest ABL and is not consistent with the description of ABL depths in lines 238:243

Response: We are sorry for this mix-up. The value provided in the manuscript was indicative of the general surface air temperature encountered in that location. The actual values during the flight period, however, were different and this is now provided in the revised manuscript:

<u>Line nos. 210-213</u>: "The meteorological conditions across the IGP during the campaign period was generally hot (surface temperature, T ~ 34.7 ± 2.8 ºC at JDR, 39 ± 1.9 ºC at VNS and 32.8 ± 3.6 ºC at BBR at the time of flight take off), with low to moderate relative humidity (RH) at JDR (RH ~ 40%) and VNS (RH ~ 60%)."

<u>Line nos. 254-255</u>: "The mean ABL heights are 1.3 ± 0.5 km, 2.3 ±0.5 km and1.4 ± 0.2 km for JDR, VNS, and BBR respectively (Vaishya et al., 2018) at local noon time."

References:

GAINS, Greenhouse Gas and Air Pollution Interactions and Synergies - South Asia Program. International Institute of Applied Systems Analysis, Laxenburg, Austria, 2010.

Guttikunda, S.K. and Jawahar, P.: Atmospheric emissions and pollution from the coal-fired thermal power plants in India, Atmos. Env. 92, 449-460 http://dx.doi.org/10.1016/j.atmosenv.2014.04.057, 2014.

Hopkins, R. J., Tivanski, A.V., Marten, B.D., and Gilles, M. K., Chemical bonding and structure of black carbon reference materials and individual carbonaceous atmospheric aerosols, J. Aerosol Sci. 38, 573–591, 2007.

Sahu, S.K., Ohara. T., and Beig, G.: The role of coal technology in redefining India's climate change agents and other pollutants Environ. Res. Lett. 12, 105006, https://doi.org/10.1088/1748-9326/aa814a, 2017.

Tiwari, M.K., Bajpai, S., Dewangan. U.K., Environmental Issues in Thermal Power Plants – Review in Chhattisgarh Context, J. Mater. Environ. Sci. 10(11), 1123-1134, 2019.

Venkataraman., C., Brauer, M., Tibrewal, K., Sadavarte, P., Ma, Q., Cohen, A., Chaliyakunne, S., Frostad, J., Klimont, Z., Martin, R.V., Millet, D.B., Philip, S., Walker, K., and Wang, S.: Source influence on emission pathways and ambient PM2:5 pollution over India (2015–2050), Atmos. Chem. Phys., 18, 8017–8039, https://doi.org/10.5194/acp-18-8017-2018, 2018

Vipradas, M., Babu, Y.D., Garud, S., and Kumar, A., Preparation of road map for mainstreaming wind energy in India, TERI project report No. 2002RT66, The Energy and Resources Institute, 2014.

—END—

Response to Reviewer-3

The paper presents the results of the aircraft in situ measurements carried out at three selected locations in the Indo Gangetic plains (IGP) in the summer of 2016 before the advent of the South West Asian Monsoon to obtain the vertical distribution of composite aerosols and Black Carbon (BC). The aim of the experiment was to distinguish the characteristics of aerosols in the vertical column from surface to peak aircraft altitude. The location and timing of the experiment was so conceived that it covers the west east cross section of the IGP from the semi-arid desert in the west, the central IGP characterized by significant anthropogenic activity and the east coast location influenced by the marine environment and industrial activity. Some other aspects investigated during the SWAAMI are already in the public domain. The well-planned experiment reveals that in-spite of the known east west heterogeneity in aerosol characteristics in the IGP as unveiled from ground-based observations, the coarse mode concentration and coarse mode mass fraction of aerosols representing mainly soil dust increases with increase in altitude across the IGP especially above the well mixed layer. Hence, the mode radii and geometric mean radii of aerosol particles increase with height. The east west heterogeneity is mainly restricted to within the boundary layer e.g. the highest coarse mode mass fraction (of the total aerosol load) is seen in the western IGP and highest accumulation mode mass fraction in the central IGP. The high concentration of coarse mode fraction is attributed to mineral dust loading. Simultaneous International Space Station overpass measurement reveals that dust aerosols reach altitude as high as 5 km in this season. On the contrary, BC mass concentration shows very little altitude variation upto the aircraft top height. The results so obtained are new, and significant from the point of view of aerosol-radiation interaction and aerosol-cloud interaction. It also establishes unequivocally for the first time the heterogeneity between aerosols within the ABL and free troposphere in the IGP. In view of the above, I strongly believe that the paper qualifies for publication in the prestigious journal ACP. I recommend publication of the article with minor revisions.

We appreciate the summary observations of the reviewer and the subsequent recommendation on the manuscript. We have addressed to all the queries/ suggestions raised by the reviewer in the revised manuscript. Our point wise response to each of the comments is given below.

Minor comments/suggestions

1. Though the paper is well written I would suggest a thorough editing of the text by the authors for more clarity at some points and inadvertent grammatical mistakes or overwrite. Also, chronology in references inside the text should be maintained throughout the text.

   Complied with. We have made a thorough revision of the text and grammatical issues in the manuscript. We have also taken care of the references, arranging in chronological order.

2. How the hygroscopic growth under extremely humid conditions as in case of BBS are taken care of in the APS measurement, please specify in the relevant text.

"The TSI-APS (3321) is suitable for operating at 10 to 90% RH (non-condensing) and 10-40°C ambient temperature. For BBR it is likely that aerosols grew under high RH conditions but might have also shrunk due to higher instrument temperature as compared to ambient. However, more controlled laboratory experiments are required to ascertain the response of the APS to hygroscopic growth of particles."

The above information is included in the revised manuscript, Line nos. 177-181.

3. The main concern regarding a few figures and their captions as given below.

a. Figure 1: Caption please re-write. It is the AOD 500 nm which is shown in the surface plot upon which the stations are marked. In the figure, the triangles may be identified with the abbreviated station names for better visibility. Authors may rethink about Figure 1, as not much discussion on it is found in the text. Figure 2 is sufficient to represent the site description with the base stations. Otherwise, a few lines on AOD distribution may be added in the text based on Figure 1.

Response: Complied with

b. Rewrite the figure caption 4.

Response: Complied with.

c. Figure 5: Replace . . . 'eastern part of India by '. . .. . ..eastern part of IGP'.

Response: Complied with.

d. Figure 8, Caption please delete 'distinct': also replace 200 by 2000

Response: Complied with.

e. Figure 11b replace MBC by FBC, perhaps there is some confusion with Fig. S2.

Response: Complied with. The figure caption is corrected.

f. Figure 12. Please zoom in the areas between the ellipse for clarity of the aircraft tracks. Also interchange b & c in the caption.

Response: A zoom in view of the flight tracks is shown (Figure-13R1) in the revised manuscript. Figure caption is corrected.

g. Figure 15 What is indicated by the vertical dashed line? Please mention in the caption.

Response: Complied with. Thanks for pointing out the error on the vertical lines, which are properly set in the revised figure (Figure-16R1) and details are included in the caption.

4. In continuation to comment 1, following are a few suggestions in the text.

a. Line 90: correct ". . .various aerosol properties" as ". . .various aerosol parameters".

Response: Complied with.

b. Line 93: modify as . . . (Bhubaneswar (BBR), the industrialized coastal location in the eastern end of the IGP.

Response: This sentence is removed as was repeating with the sentence in line no 111-125.

c. Line 90-95 can be merged with Line no 111-120 and figure 1 can be shifted to this section.

Response: Lines 90-95 is modified considering the repeating information with lines 111-120. Figure-1 is shifted to this section.

d. Line: 96-99: Please rewrite the sentence

Response: Complied with, the sentence is modified.

e. Line 103-110: can be placed at the end of this section or can be shifted to section 2.2

Response: Complied with, the lines are shifted to section 2.2

f. Line 138-146: Should be rewritten and placed at Line 131.

Response: Complied with. These lines are rewritten and shifted as suggested.

<u>Line nos. 127-134</u>: " Figure-2a shows the actual dates of onset of the monsoon at different parts of India in 2016. As can be seen from the figure, despite a delayed onset at the southern tip of India, monsoon advanced fast in to the central/northern parts of India. Yet, all the flight sorties from the respective base stations were completed ahead of the advent of monsoon to that station. At the eastern IGP, the aircraft sorties were made from 'BBR' before the onset of monsoon over India; at 'VNS', the flights were conducted while monsoon advanced only to the central peninsula. The final sets of sorties were conducted at 'JDR' when the monsoon covered most of the central and eastern part of India, but yet to progress towards northwestern parts."

g. Section 2.4 should be merged with section 2.2 or put before section 2.3.

Response: Complied with.

h. Line 287-292: See if these sentences are more appropriate to place in previous paragraph (after Line 271)

Response: Complied with.

i. Line 349: '. . .. . organic carbon being strong absorbers of UV radiation', please check.

Response: Complied with. We have modified the sentence as

<u>Line nos. 357-359</u>: " Higher values of AAOD at 388 nm are indicative of the presence of dust or biomass burning aerosols. This is because absorption by dust and organic carbon from biomass burning sources have strong wavelength dependency with higher absorption at near-UV wavelengths."

j. Line 503: Rewrite the sub-section heading

Response: Complied with. We have modified the section heading as "Inter-seasonal variability: a case study at JDR".

—END—

Air-borne in-situ measurements of aerosol size distributions and BC across the IGP during SWAAMI--RAWEX

Mukunda Madhab Gogoi[1], Venugopalan Nair Jayachandran[1], Aditya Vaishya[2], Surendran Nair Suresh Babu[1], Sreedharan Krishnakumari Satheesh[3,4] and Krishnaswamy Krishna Moorthy[3]

[1]Space Physics Laboratory, Vikram Sarabhai Space Centre, Thiruvananthapuram – 695022, India
[2]School of Arts and Sciences, Ahmedabad University, Ahmedabad – 380009, India
[3]Centre for Atmospheric and Oceanic Sciences, Indian Institute of Science, Bengaluru – 560012, India
[4]Divecha Centre for Climate Change, Indian Institute of Science, Bengaluru – 560012, India

Abstract

During the combined South-West Asian Aerosol Monsoon Interaction (SWAAMI) – Regional Aerosol Warming Experiment – experiment(SWAAMI -RAWEX), collocated air-borne measurements of aerosol number-size distributions in the size (diameter) regime 0.5 to 20 µm and black carbon (BC) mass concentrations were made across the Indo-Gangetic Plains (IGP), for the first time, from three distinct locations, just prior to the advent of Indian Summer Monsoon over the IGP. These measurements provided an east-west transect of region-specific properties of aerosols as the environment transformed from mostly-arid conditions of western IGP (represented by Jodhpur, JDR) having dominance of natural aerosols to the Central IGP (represented by Varanasi, VNS) having very high anthropogenic emissions, to the eastern IGP (represented by the coastal station Bhubaneswar, BBR) characterized by a mixture of the IGP outflow and marine aerosols. Despite these, the aerosol size distribution revealed an increase in coarse mode concentration and coarse mode mass-fraction (fractional contribution to the total aerosol mass) with the increase in altitude across the entire IGP, especially above the well-mixed region. Consequently, both the mode radii and geometric mean radii of the size distributions showed an increase with altitude. However, near the surface and within the atmospheric boundary layer (ABL), the features were specific to the different sub-regions; with the highest coarse mode mass fraction (F_{MC} ~72%) in the western IGP and highest accumulation fraction in the Central IGP with the eastern IGP coming in-between. The elevated coarse mode fraction is attributed to mineral dust load arising from local production as well as due to advection from the west. This was further corroborated by data from Cloud Aerosol Transportation System (CATS) onboard International Space Station (ISS), which also revealed that the vertical extent of dust aerosols reached as high as 5 km during this period. Mass concentrations of Black Carbon (BC) were moderate (~1 µg m^{-3}) with very little altitude variation up to 3.5 km, except over in the Central IGP (VNS) where very high concentrations were seen near the surface and within the ABL. BC induced atmospheric heating rate was highest near the surface at VNS (~ 0.81 K day^{-1}), while showing an increasing pattern with altitude at BBR (~ 0.35 K day^{-1} at the ceiling altitude).

Keywords: Aerosol size distribution profile, BC mass fraction, aerosol type, IGP, monsoon, SWAAMI

Corresponding Author:
Dr. Mukunda M. Gogoi
Scientist
Space Physics Laboratory, Vikram Sarabhai Space Centre
Indian Space Research Organization, Thiruvananthapuram – 695022, India

Email: dr_mukunda@vssc.gov.in
Phone: +91-471-256 3365; Fax: +91-471-270 6535

1. Introduction

The Indo-Gangetic Plains (IGP) remains one of the global hotspots of aerosols. The prevailing high aerosol loading and the relative abundance of its constituents (being a mixture of natural and anthropogenic species) is known to show significant seasonality (~~Rana et al., 2019; Vaishya et al., 2018; Brooks et al., 2018~~2019; ~~Moorthy et al., 2016;~~ Gautam et al., 2011; Praveen et al., 2012; Moorthy et al., 2016; Vaishya et al., 2018; Rana et al., 2019; Brooks et al., 2019 ~~Gautam et al., 2011~~). This arises due to combined effects of the dense population and the associated anthropogenic and industrial activities, as well as the loose alluvial soil of this regions having vast semi-arid and arid characteristics to the west. A dense network of thermal power-plants, several of them being coal fired, is among the prominent source of anthropogenic emissions over the region. This is abetted by the synoptic meteorology with its strong seasonality (Gautam et al., 2010; Nath et al., 2018; Singh et al., 2018~~; Gautam et al., 2010~~) and the orography that slopes down from the west to east bound on the north and south respectively by the Himalayas and the Aravalli ranges and Bihar Plateau forming a confined channel (Moorthy et al. 2007; Gogoi et al., 2017). For accurate quantification of the radiative implications of this complex aerosol system, several concerted studies have been made using ground based (~~Bansal et al., 2019;~~ Giles et al., ~~2011~~2012; Bansal et al., 2019) and space-borne measurements (~~Kumar et al., 2018; Srivastava, 2016;~~ Mhawish et al., 2017; Kumar et al., 2018 ~~Srivastava, 2016~~) as well as numerical modeling (Govardhan et al., 2019). However, most of these studies have uncertainties arising out of the ill-represented altitude variation of aerosol properties due to sparse measurements. Height resolved in-situ measurements of aerosol properties are indispensable not only in this regard, but also for understanding aerosol-cloud interactions.

In recent years, a few campaign-mode airborne measurements have been made over this region to estimate the altitude-resolved properties of aerosols that are important in aerosol-radiation interactions (~~Gogoi et al., 2019; Vaishya et al., 2018;~~ Padmakumari et al., 2013; Babu et al., 2016; Nair et al., 2016; Vaishya et al., 2018; Gogoi et al., 2019 ~~Padmakumari et al., 2013~~). These include the measurements of aerosol scattering and absorption coefficients conducted as part of the Regional Aerosol Warming Experiment (RAWEX; Babu et al., 2016) to delineate the spatio-temporal variability in the altitude distribution of aerosol single scattering albedo (SSA) across the IGP during winter and pre-monsoon seasons and aerosol and cloud parameter measurements conducted as part of the Cloud Aerosol Interaction and Precipitation Enhancement Experiment (CAIPEEX; ~~Konwar et al., 2015~~ Kulkarni et al., 2012). Some studies have also reported significant contribution of dust and BC ~~as~~to the elevated aerosol load (~~Pandey et al., 2016; Li et al.,~~

2016;~~ Praveen et al., 2012; Kedia et al., 2014; Pandey et al., 2016; Li et al., 2016;~~) and their potential role to act as ice nuclei (Padmakumari et al., 2013). However, despite its importance in radiative interactions and CCN activation, the altitude-resolved measurements of aerosol size distribution are extremely sparse, or non-existent, especially just prior to the onset of the Indian Summer Monsoon, when the sources of aerosols, their mixing and transport pathways are all complex. The information on aerosol size distribution is important for accurately describing the phase function, which describes the angular variation of the scattered intensity. The knowledge of its vertical variation would thus improve the accuracy of ARF estimation and hence heating rates. Such information is virtually non-existing over this region. Further, the knowledge of the variation of size distribution with altitude would be useful in better understanding the aerosol-cloud interactions and CCN characteristics, during the evolving and active phase of the Indian monsoon. This was among the important information aimed to be obtained under SWAAMI - RAWEX (~~South West Asian Aerosol Monsoon Interactions;~~ https://gtr.ukri.org/projects?ref=NE%2FL013886%2F1 and http://www.spl.gov.in/SPL/index.php/arfs-research/field-campaigns/asfasf) - a joint Indo-UK field experiment involving airborne measurements using Indian and UK aircrafts during different phases of the Indian monsoon, right from just prior to the onset of monsoon (i.e. in the beginning of June).

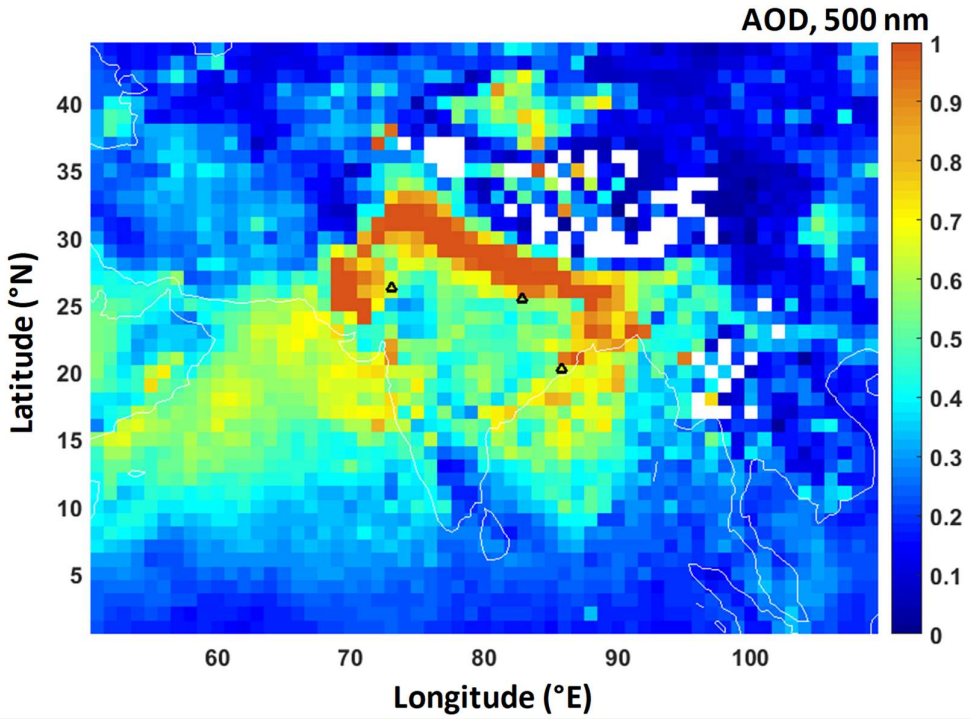

Figure-1: Three distinct base stations: (i) 'Jodhpur (JDR; 26.25°N, 73.04°E)' in the western IGP, (ii) 'Varanasi (VNS; 25.44°N, 82.85°E)' in the central IGP and (iii) 'Bhubaneswar (BBR; 20.25°N, 85.81°E)' in the eastern coastal IGP, from where the aircraft measurements were conducted during 01-20 June 2016. The background colour is indicative of the mean AOD at 550 nm during the study period obtained from MODIS sensor (MOD08_D3_6.1, Dark-Target and Deep-Blue combined mean) on-board Terra satellite.

During this campaign, vertical profiles of various aerosol properties parameters have been measured using an instrumented aircraft from three base stations – Jodhpur (JDR), representing the semi-aridwestern, central and eastern end of the IGP; Varanasi (VNS), representing central IGP characterizedby significant anthropogenic activities; and the industrializedcoastal location in the eastern end of the IGP(Bhubaneswar, BBR) – during 01 to 20 June 2016,just prior to the onset of the Indian summer monsoon. Some important results on the optical and CCN characteristics are already reported (Vaishya et al., 2018; Jayachandran et al 20192020). In the present study, we have examined the vertical profiles of aerosol number-size distributions in the size (diameter) regime 0.5 to 20 µm and black carbon (BC) mass concentrations, across the IGP(Figure 1),based on the measurements over western, central and eastern IGP from base stations shown in the figure. The results are presented and discussed in the light of other supplementary information.

2. Experimental Details and database

2.1 Study region and flight details

The measurements were carried out aboard the instrumented aircraft (Beechcraft 200) fitted with an iso-kinetic inlet, mounted (front facing) at the bottom of the fuselage for aspirating ambient aerosols and detailed in a few earlier papers (Babu et al., 2016; Vaishya et al., 2018; Gogoi et al., 2019). A constant volumetric flow of 70 LPM (liters per minute) was maintained using an external pump connected to the main inlet assembly, which provided iso-kinetic flow for the average speed of 300 km/hr maintained by the aircraft during the entire campaign. The efficiency of this inlet system has been already proven in several previous campaigns (Gogoi et al., 2019; Nair et al., 2016; Babu et al., 2016).

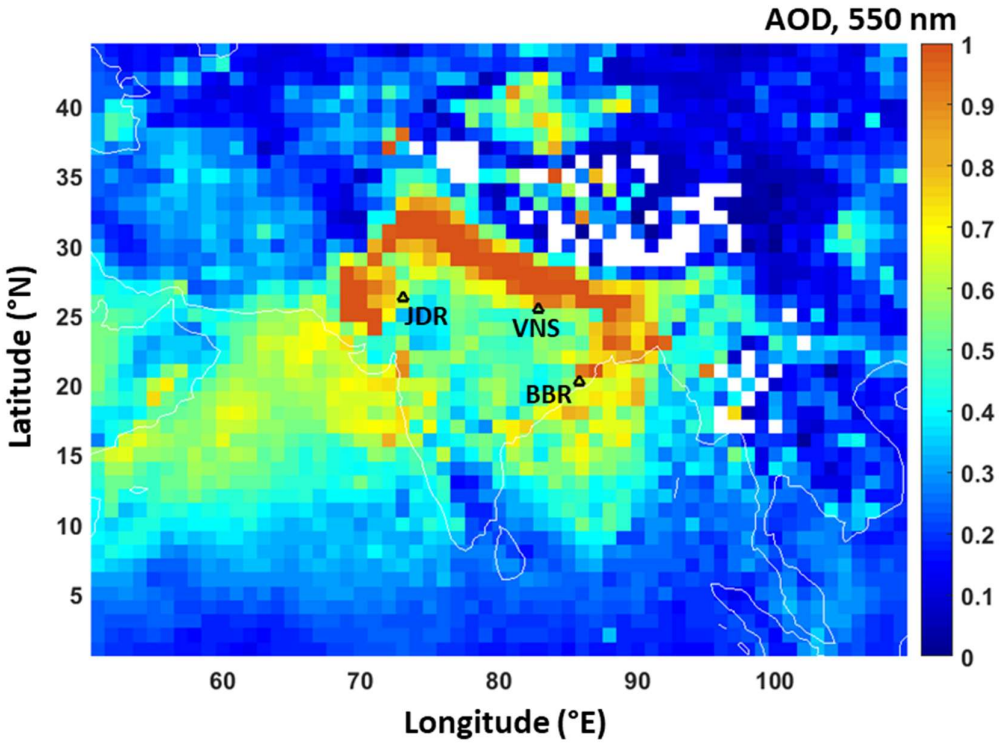

Figure-1: Three distinct base stations: (i) 'Jodhpur (JDR; 26.25°N, 73.04°E)' in the western IGP, (ii) 'Varanasi (VNS; 25.44°N, 82.85°E)' in the central IGP and (iii) 'Bhubaneswar (BBR; 20.25°N, 85.81°E)' in the eastern coastal IGP, from where the aircraft measurements were conducted. The spatial map of AOD at 550 nm obtained from MODIS sensor (MOD08_D3_6.1, Dark-Target and Deep-Blue combined mean) on-board Terra satellite during the study period (01-20 June 2016) is shown in the background.

The base stations (Figure-1), from where the aircraft operations were carried out, represented distinct regions of the IGP; 'Jodhpur (JDR; 26.25°N, 73.04°E)' in the western IGP is an arid/ semi-arid region with low urban activities, lying downwind the 'Great Indian Desert' to its west (JDR has population density of 161 per sq. km).'Varanasi (VNS; 25.44°N, 82.85°E)' in the central IGP is located downwind of Jodhpur, characterized by extensive anthropogenic activities (automobiles, small and large-scale industries and thermal power plants and wide spread agricultural activities) by its dense population (density 2,399 km^{-2}). 'Bhubaneswar (BBR; 20.25°N, 85.81°E)' is an urban location in the eastern IGP (population density of 2131 km^{-2}), and experiences the influence of marine aerosol component from the Bay-of-Bengal (~ 50 km away from the base station) in addition to the influence of IGP outflow and local aerosol sources from nearby thermal (coal based) power plants, mining and fertilizer based industries etc. (Panda et al., 2016). The

northwestern part of India has an undulating topography, due to which monsoon currents loose moisture while crossing the western mountain ranges (Aravalli) and results in dry arid regions (Moorthy et al., 2007). Strong dust-rising winds are a common feature of the IGP in general and its western parts in particular during April to July (Banerjee et al. 2019). In the central IGP, ~~Varanasi~~ VNS and its environs holds largely even topography, where the Ganga is the principal river. In the eastern IGP, BBR is topographically decorated with western uplands and eastern lowlands, with hillocks in the western and northern parts. These base stations, thus provided a west-east cross section of the highly aerosol laden IGP; where the aerosol characteristics are known to change longitudinally. The spatial map of AOD at 550 nm (Figure-1) clearly shows the existence of higher aerosol loading (AOD > 0.5) over the observational site during the study period.

~~The present study thus provides altitude resolved information on aerosols across the IGP, just prior to the onset of monsoon over the region.~~ ~~The geographical positions of the three base stations, along with the~~ Figure-2a shows the actual dates of onset of the monsoon at different parts of India in 2016~~ are shown in Figure 2a~~. As can be seen from ~~it~~the figure, despite a delayed onset at the southern tip of India, monsoon ~~made a~~ advanced fast ~~advance~~in to the central/northern parts of India. Yet, all the flight sorties from the respective base stations were completed ~~well~~ ahead of the advent of monsoon to that station. At the eastern IGP ~~'BBR'~~, the aircraft sorties were made from 'BBR'~~during 01-05 June 2016 when~~ before the onset of monsoon ~~has not yet set in~~ over India; at 'VNS', the flights were conducted ~~during 08-13 June 2016,~~ while monsoon ~~has~~ advanced only to the central peninsula. ~~By 19 June 2016, the southwest monsoon has covered most of the central and eastern part of India, but yet to progress towards northwester parts and the~~ The final set of sorties were conducted at 'JDR' when the monsoon covered most of the central and eastern part of India, but yet to progress towards northwestern parts.~~during 17-20 June 2016;thereby providing altitude resolved information on aerosols across the IGP, just prior to the onset of monsoon over the region.~~

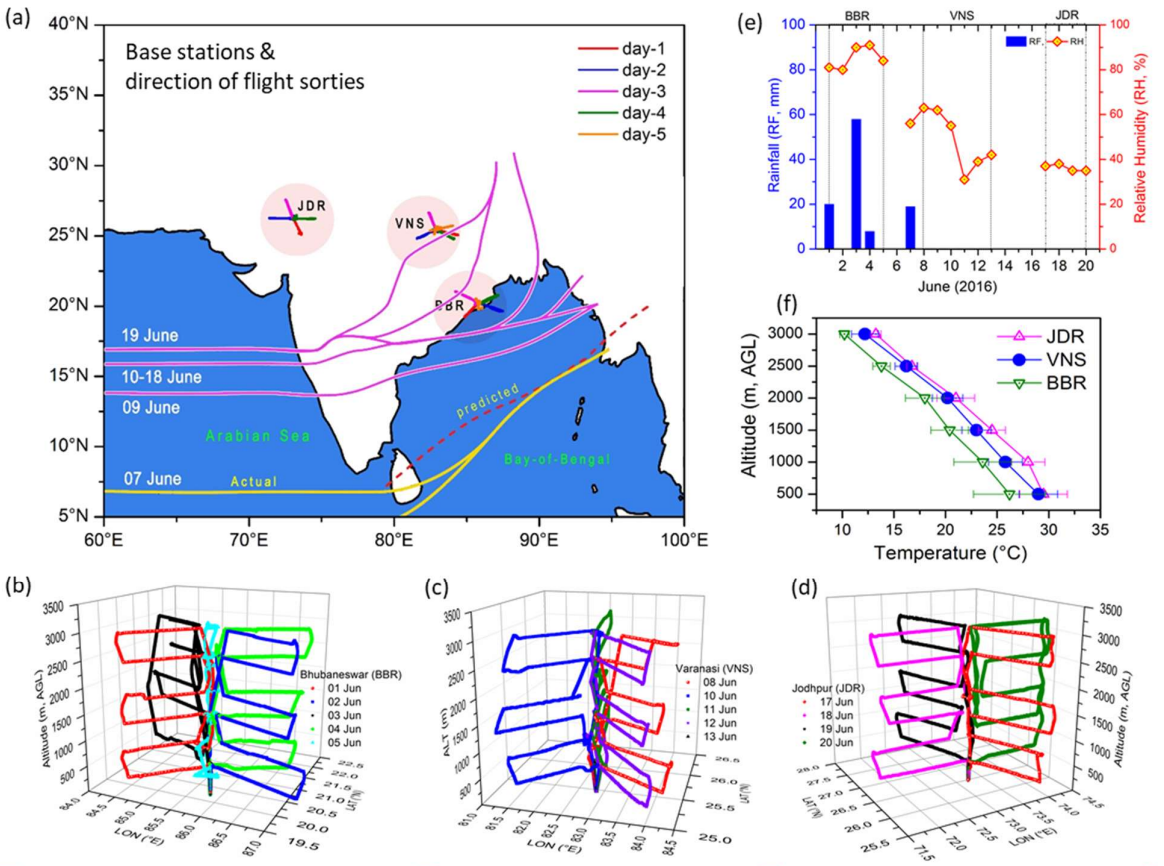
(a)
Base stations &
direction of flight sorties
day-1
day-2
day-3
day-4
day-5
JDR
VNS
BBR
19 June
10-18 June
09 June
07 June
Actual
predicted
Arabian Sea
Bay-of-Bengal
(e)
BBR
VNS
JDR
RF
RH
Rainfall (RF, mm)
Relative Humidity (RH, %)
June (2016)
(f)
JDR
VNS
BBR
Altitude (m, AGL)
Temperature (°C)
(b)
Bhubaneswar (BBR)
01 Jun
02 Jun
03 Jun
04 Jun
05 Jun
(c)
Varanasi (VNS)
08 Jun
10 Jun
11 Jun
12 Jun
13 Jun
(d)
Jodhpur (JDR)
17 Jun
18 Jun
19 Jun
20 Jun

171

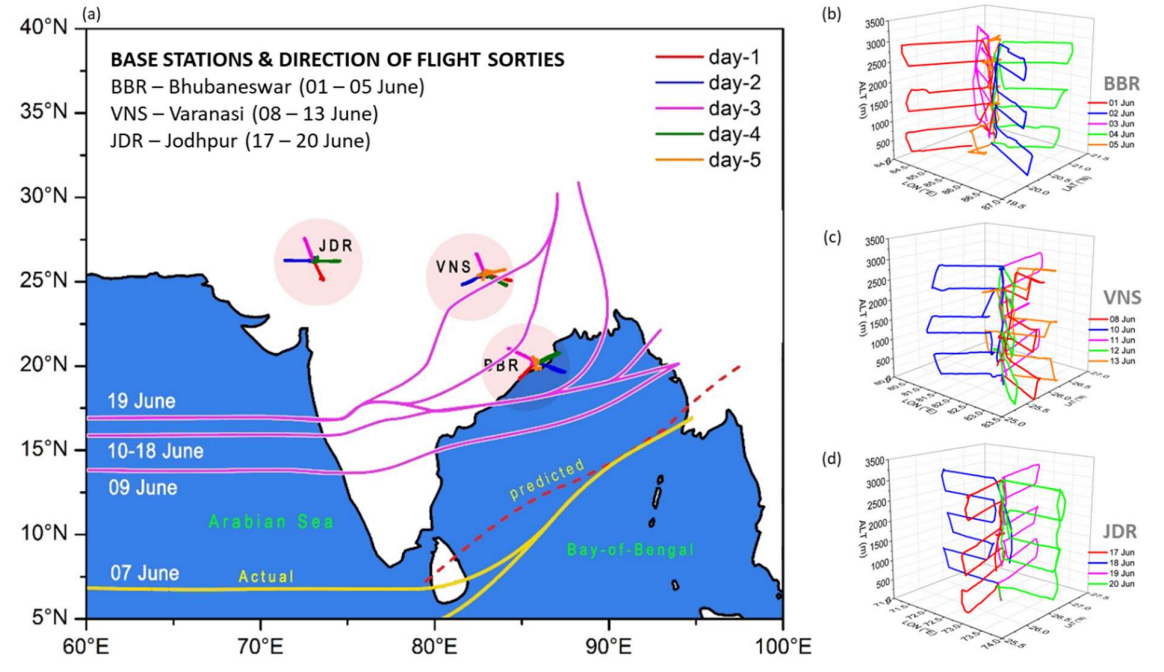
(a)
BASE STATIONS & DIRECTION OF FLIGHT SORTIES
BBR – Bhubaneswar (01 – 05 June)
VNS – Varanasi (08 – 13 June)
JDR – Jodhpur (17 – 20 June)
day-1
day-2
day-3
day-4
day-5
JDR
VNS
BBR
19 June
10-18 June
09 June
07 June
Actual
predicted
Arabian Sea
Bay-of-Bengal
(b)
BBR
(c)
VNS
(d)
JDR

172

Figure-2: (a) ~~The base stations in the northern part of India.~~ The onset (actual) of SW-Monsoon at different parts of India, ~~is also~~ shown ~~in the figure~~ by the yellow and pink (solid) lines. Horizontal and vertical flight paths during each of the sorties at ~~(b) Jodhpur (JDR), (c) Varanasi (VNS) and (d~~b) Bhubaneswar (BBR), (c) Varanasi (VNS) and (d) Jodhpur (JDR)~~:.(e) Daily rainfall (total) and relative humidity (mean) during the period of observation; (f) vertical profiles of mean ambient temperatures.~~

~~As can be seen from it, despite a delayed onset at the southern tip of India, monsoon made a fast advance. Yet, all the sorties from the respective base stations were completed well ahead of the advent of monsoon to that station.At the eastern IGP 'BBR', the aircraft sorties were made during 01-05 June 2016 when monsoon has not yet set-in over India; at 'VNS', the flights were conducted during 08-13 June 2016, while monsoon has advanced only to the central peninsula. By 19 June 2016, the southwest monsoon has covered most of the central and eastern part of India, but yet to progress towards northwester parts and the final set of sorties were conducted at 'JDR' during 17-20 June 2016; thereby providing altitude-resolved information on aerosols across the IGP, just prior to the onset of monsoon over the region.~~

From each of the ~~above~~ base stations, 4 to 5 sorties were carried out on successive days in different horizontal directions about the station, as shown by the ground projections (horizontal lines in Fig 2a), with a view to obtain~~ing~~ an average sub-regional representation in the shortest time possible. During each of the sorties, measurements were made at six discrete levels following a staircase configuration as shown in Figure 2 b-d (for JDR, VNS and BBR respectively). Accordingly, the aircraft initially climbed to the base/ceiling altitude, stabilized and made horizontal flight along the projected track for about 30 min before climbing up/ down to the next higher/ lower levels and stabilizing. This procedure was repeated for all levels (~ 0.5, 1, 1.5, 2, 2.5 and 3 km a.g.l.) until the last level. The ceiling altitude was restricted to 3.5 km based on the unpressurised mode of operation of the aircraft. All the flights were carried out around mid-day ~~so that~~ since thorough vertical mixing is established by the daytime convective boundary layer eddies.

2.2. On-board Instrumentation

The measurements were carried out aboard the instrumented aircraft (Beechcraft-200) fitted with an iso-kinetic inlet, mounted (front facing) at the bottom of the fuselage for aspirating ambient aerosols and detailed in ~~a few~~ earlier papers (Babu et al., 2016; Vaishya et al., 2018; Gogoi et al., 2019). A constant volumetric flow of 70 LPM ~~(liters per minute)~~ was maintained using an external pump connected to the main inlet assembly, which provided iso-kinetic flow for the average speed

of 300 km/hr maintained by the aircraft during the entire campaign. The efficiency of this inlet system has been already proven in several previous campaigns (Babu et al., 2016; Nair et al., 2016; Gogoi et al., 2019).

Measurement of aerosol size distribution

A factory-calibrated, Aerodynamic Particle Sizer (APS) spectrometer (TSI, Model: 3321) is used for the measurement of aerosol size distribution. It measures size-resolved number concentration of the ambient aerosols in the size range from 0.5 to 20 μm, over 52 channels spaced equally in logarithmic size bins; at a sampling frequency of 1 minute. Aerosol particles in this size range is most important in influencing the optical (scattering and extinction) and CCN and ice nuclei (IN) characteristics.

The APS measures the concentration of particles in terms of their aerodynamic diameters by comparing the velocity of particle (controlled by an accelerating flow field) to that of a unit density sphere having same velocity. Particle velocity is estimated from the measurement of time of flight (Mitchell and Nagel, 1999). In the present study a sheath flow at 4 LPM (litres per minute) was maintained against the sample flow of 1 LPM. The instrument automatically adjusts the flow rates with changes in ambient pressure to maintain the specified flow rates. Occasionally, when the aircraft passes through clouds, the aerosol number concentration shot up from the otherwise stable values. Such outliers are removed following 2σ criteria, wherein data points at a particular level lying outside 2σ values of the level-average were removed. The number of such screened out points were < 3% of the total. The consistency in the flow was periodically checked each time, before start of measurements from the new base station. Similarly, the optical components and tubing of the system were cleaned immediately after moving to a new base station.
The TSI-APS (3321) is suitable for operating at 10 to 90% RH (non-condensing) and 10 - 40 °C ambient temperature. For BBR, it is likely that aerosols grew under high RH conditions but might have also shrunk due to higher instrument temperature as compared to ambient. However, more controlled laboratory experiments are required to ascertain the response of the APS to hygroscopic growth of particles.

Measurement of Black Carbon aerosols

Mass concentration of ambient BC aerosols was estimated using a 7-channel aethalometer (Model: AE-33, Magee Scientific, USA), which measures the attenuation of light that passes through the

aerosol laden filter at wavelengths 370, 470, 520, 590, 660, 880, and 950 nm. The loading (or shadowing) effect arising out of the successive deposition of aerosols in the filter media is automatically compensated in real-time in the new-generation Aethalometer; while the multiple scattering effects were~~as~~ minimised by using advanced filter tape material (Drinovec et al.,2015). ~~During the measurement~~In the present study, BC mass concentrations were obtained ~~in each~~ at 1 minute interval by operating the aethalometer ~~was set for~~ at 50% of the maximum attenuation,~~to reduce the 'shadowing effect' (Weingartner et al., 2003)~~, and a standard mass flow rate of 2 LPM ~~and time base of 1 min.~~ under standard temperature (T_O, 293 K) and pressure (P_O, ~~1017~~1013 hPa). As the unpressurised aircraft climbed higher, the instrument experienced ambient pressure (P) and temperature (T). In order to maintain the set mass flow, the pumping speed of the instrument was automatically increased (through internal program) to aspire more volume of air. However, the volume of air aspirated at ambient pressure and temperature requires to be corrected to standard atmospheric condition for the actual estimate of BC (Moorthy et al., 2004). Thus, the actual volume of air aspirated by the Aethalometer at different atmospheric level is,

$$V = V_o \frac{P_o T}{P T_o}$$

Thus, ~~The effect of air pressure variation with altitude on the measurements was corrected following Moorthy et al., (2004) to estimate the~~ true BC mass concentration (M_{BC}) is

$$M_{BC} = M^*_{BC} \left[\frac{P_O T}{P T_O}\right]^{-1} \quad (1)$$

where M^*_{BC} is the instrument measured raw mass concentration of BC at ambient ~~conditions, $P_0$and P are the standard and ambient~~ pressure and ~~$T_0$and T are the corresponding~~ temperatures. Details of the aethalometer principle, operation, uncertainty involved and error budget are reported in several earlier literatures (~~Gogoi et al., 2017;~~ Weingartner et al., 2003; Arnott et al., 2005; Gogoi et al., 2017). In general, the instrumental uncertainty ranges from 50% at 0.05 µg m^{-3} to 6% at 1µg m^{-3} (Corrigan et al., 2006) and the uncertainty in the estimation of absorption coefficients is around 10% (Vaishya et al., 2018).

2.4. General synoptic meteorology during the campaign

The meteorological conditions across the IGP during the campaign period was generally hot (surface temperature, T ~ 34.7 ± 2.8 ºC at JDR, 39 ± 1.9 ºC at VNS and 32.8 ± 3.6 ºC at BBR at the time of flight take off), with low to moderate relative humidity (RH) at JDR(RH ~ 40%) and

VNS (RH ~ 60%). The values of RH at BBR was relatively higher (as high as 80%) associated with its coastal proximity, in addition to the influence of ~~with~~ mild pre-monsoon rainfall during the first (01-June-2016; light rain during noon), third (03-June-2016; heavy rain ~ 60 mm in the night) and fourth (04-June-2016; light rain in the morning and during noon) days of observations. The records of T and RH were obtained from the sensors on-board the aircraft, while the rainfall data was obtained from the airport meteorological department at BBR.

2.3. Supplementary data

Supplementary data used in this study include aerosol backscattering coefficients and depolarization ratio measured by the *Cloud Aerosol Transportation System* (CATS) aboard the International Space Station (ISS). The CATSis a comprises of an elastic backscatter lidar consisting of two high repetition rate (4-5 kHz), low energy (1-2 mJ) Nd:YVO_4 lasers operating at three wavelengths (1064, 532, and 355 nm). The receiver subsystem consists of a 60 cm telescope having a 110 micro-radian field of view, photon-counting detectors, and associated control electronics (Yorks et al., 2014; 2016).As the altitude of ISS orbit is about 405 km (51-degree inclination), CATS provides a comprehensive coverage of the tropics and mid-latitudes, with nearly a three-day repeat cycle. Level 2 data of CATS (https://cats.gsfc.nasa.gov/data/) are used (Lee et al., 2018) in the present study, which provides the geophysical parameters, such as the vertical feature mask, profiles of cloud and aerosol properties (i.e. extinction, particle backscatter), and layer-integrated parameters (i.e. lidar ratio, optical depth). In addition, types of aerosols are also derived based on CATS typing algorithms where eight aerosol types (in CATS mode 7.1) are identified: volcanic, dust, dust mixture, clean/background, polluted marine, marine, polluted continental and smoke. Incorporating the information of backscatter color ratio (1064/532-nm) and spectral depolarization (ratio of perpendicular to parallel backscatter) ratio(1064/532-nm), Mode 7.1 provides the characteristic of aerosol regimes (York et al., 2016) as below:

Table-1: Classification of aerosol types for CATS mode 7.1 (York et al., 2016).

Aerosol Type	Aerosol feature base	Depolarization ratio (δ'_{1064})	Color Ratio (γ'_{1064})
Volcanic	> 10 km	-	-
Dust	< 10 km	> 0.3	-
Dust mixture	< 10 km	0.2 > δ > 0.3	-
Clean/background	< 10 km	-	< 0.0005 sr^{-1}
Polluted marine	< 10 km	$\delta'_{1064}/\ \delta'_{532} > 50\%$	$\gamma'_{532}/\ \gamma'_{1064} < 1.75$

Marine	< 10 km	$\delta'_{1064}/\ \delta'_{532} < 50\%$	$\gamma'_{532}/\ \gamma'_{1064} < 1.75$
Polluted continental	< 10 km	$\delta'_{1064}/\ \delta'_{532} > 50\%$	$\gamma'_{532}/\ \gamma'_{1064} > 1.75$
Smoke	< 10 km	$\delta'_{1064}/\ \delta'_{532} < 50\%$	$\gamma'_{532}/\ \gamma'_{1064} > 1.75$

~~2.4. General synoptic meteorology during the campaign~~

~~The general surface meteorological conditions across the IGP during the campaign period are shown in Figure 2(e-f), while the synoptic conditions are shown in Figure2(a). The daily mean values of relative humidity(Figure 2e) showed spatial variation typical to this region; varying from very high value (above 80%) at the eastern IGP(BBR) to the lowest value (~40%) at the western arid region (JDR), with values varying between 40% and 60% at VNS. The large value of relative humidity (RH)at BBR was also associated with mild pre-monsoon rainfall (Figure 2e) thereduring the first (01-June-2016; light rain during noon), third (03-June-2016; heavy rain ~ 60 mm in the night) and fourth (04-June-2016; light rain in the morning and during noon) days of observations. Similar to RH, ambient temperature (Figure 2f) also showed spatial variation being warmest atJDR followed by VNS and BBR, throughout the altitude range from the surface to ~ 3 km.~~

3. Results and discussion

3.1 Aerosol number size distributions

Aerosol number size distributions [dN/d (logDp)], representative of each of the 3 sub-regions of IGP, are presented in Figure 3; the panels from left to right representing the sub-regions JDR, VNS and BBR, from the west to east IGP.

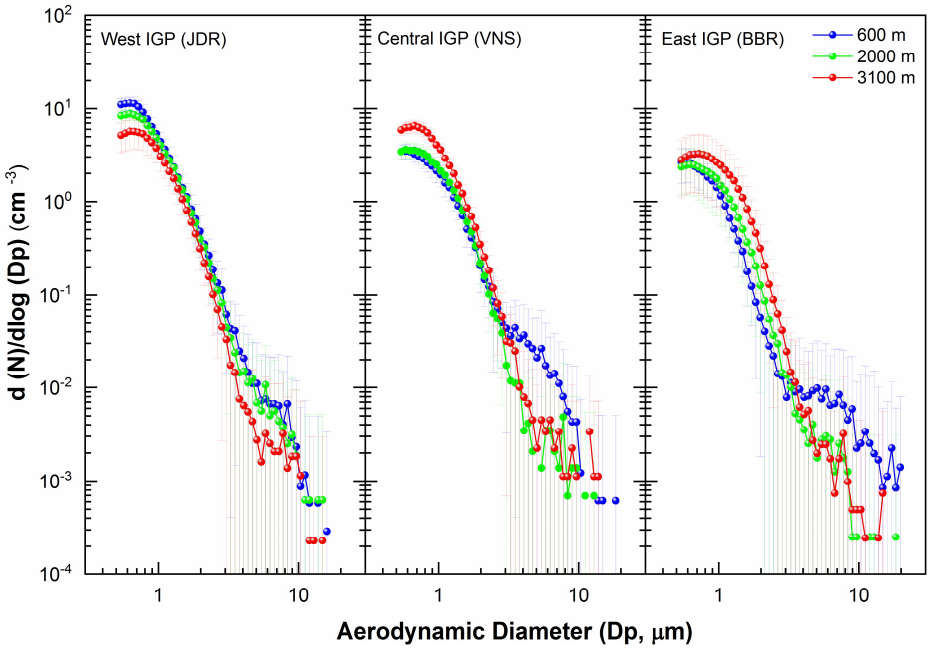

Figure-3: Aerosol number size distributions (mean profiles averaged for all the days) at three distinct altitudes of JDR, VNS and BBR, representative of (i) near the surface (600 m above ground level) having proximity to emission sources, (ii) in the upper ABL (2000 m above ground level) and (iii) in the free troposphere (3100 m). Vertical bars over the points are the ensemble standard deviations. Individual size distributions at different heights of ~ 500 m interval are given in supplementary figure-S1.

Three distributions are shown for each station, representative of (i) near the surface with proximity to emission sources (600 m AGL), (ii) in the upper ABL (2000 m AGL) and (iii) in the free troposphere (3100 m AGL) following the mean ABL heights (1.3 ± 0.5 km, 2.3 ±0.5 kmand1.4 ± 0.2 km for JDR, VNS, and BBR respectively; Vaishya et al., 2018) at local noon time. Aerosol number concentration below 0.542 µm are not size-classified and represented as a single count (between 0.3 and 0.542 µm) are shown as a function of altitude in figure 4 (a).

The figures clearly reveal that ~~over~~at all altitudes ~~and at~~ above ~~all the~~different stations, the size distributions are consistently bimodal, with a prominent accumulation mode (<1µm) and a weaker secondary mode (>1µm).The concentration of particles in the unclassified size regime (below 0.542 µm), showed a gradual decrease with increase in altitude at all stations and a spatial distinctiveness with highest near surface concentration in the Central IGP (most anthropogenically impacted sub-region of the IGP) depicting sharper altitude variation as against the other two sub-regions.

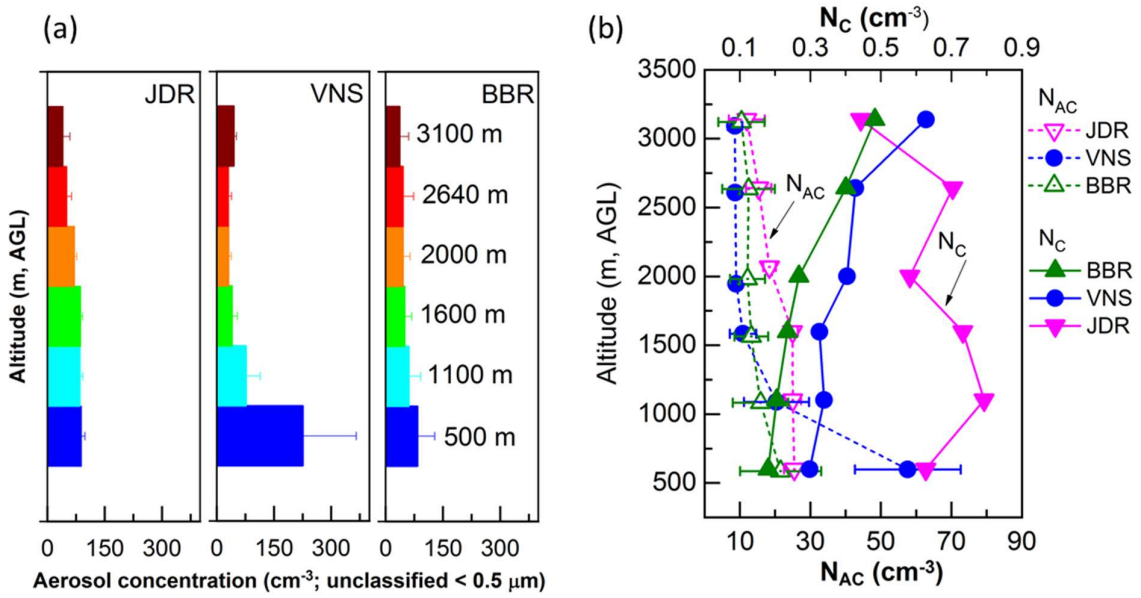

Figure-4: Vertical profiles of ~~(a) A~~aerosol number concentrations~~;in the unclassified size range ((~~a) between 0.3 and 0.54 μm (in the unclassified size range of APS); (b) ~~Vertical profiles of aerosol accumulation and coarse mode number concentrations (N_{AC}) as measured by APS~~ in the accumulation and coarse mode size range (between 0.3 and 20 μm, denoted by N_{AC}) along with coarse mode number concentrations (N_C).

As it is well-established that during pre-monsoon/ prior to the onset of monsoon, both the natural and anthropogenic aerosol species coexist in large abundance over the IGP, we examined in Figure 4b, the altitude profiles of accumulation mode aerosols (concentration below 1 μm), which are mostly attributed to be of anthropogenic origin and coarse mode aerosols (above 1 μm), which are mostly of natural origin. Accumulation mode aerosol concentration showed only weak altitudinal dependence above 1 km at all the sub-regions, though at VNS, there was a sharp increase in the concentration below 1 km, obviously due to source-proximity. This feature is seen in Figure 4a also. This observation is supported by the collocated measurements of aerosol total number concentrations (N_T) as measured by a condensation nuclei (CN) counter aboard the aircraft (Jayachandran et al., ~~2019~~2020) in the size range above 2.5 nm, showing highest values of N_T in the entire altitude range of measurements over VNS. On the other hand, the vertical profiles of coarse mode aerosol~~s~~ concentrations (N_C) showed significantly large abundance over the western IGP (arid/ semi-arid regions) represented by JDR, similar to the spring time observations reported by Gogoi et al., (2019).

These observations are also in-line with the reported values of dust fractions (Vaishya et al., 2018) during the same campaign, showing the enhancement of dust fraction from 10 to 20 % at 300 m to more than ~~around~~90 % above 2 km altitude at JDR; while smallest dust faction (< 10%) was observed at BBR in the entire altitude range. Over the central IGP, synoptic wind-driven desert dust aerosols, leads to elevated layers of aerosols having higher dust fraction (>50%). However, it should be noted that dust over the central IGP is more absorbing in nature because of its mixing with other anthropogenic emissions (such as BC; Vaishya et al., 2018), while that over western IGP is rather pristine in nature. Thus, quantification of the absolute magnitude of coarse mode aerosol concentrations is very important to understand the significance of elevated aerosol load on radiative perturbations.~~, because coarse mode dust contributes largely to aerosol scattering as well as absorption, compared to their anthropogenic counterpart, which contributes dominantly to absorption.~~

~~Another interesting feature is t~~The increasing concentration of ~~these~~ coarse mode particles with the increase in altitude across the entire IGP is another interesting feature in the present study; which is most conspicuous at the central IGP and least at the west, implying their increasing role at higher altitude; probably due to the lofted regional dust and advected mineral dust from west Asian regions.

With a view to quantifying this, the size distribution spectra are averaged for each altitude level and for each station. From these spectra, the geometrical mean diameter (Dg) is estimated as a function of altitude, using the following equation

$$D_g = exp\left[\frac{\sum_l^u n_i \, ln(D_{pi})}{N}\right] \quad (2)$$

where $D_{\mathrm{pi}}\left(=\sqrt{(D_i * D_{i+1})}\right)$denotes the geometric midpoint of each channel of the APS, n_{i} is the particle concentration in i^{th} channel and $N = \sum_l^u n_i$ is the total concentration.Accordingly, Dg of a spectrum of particles is the 50% probability point of an equivalent diameter having half of the particle concentrations larger than this size and remaining half is below that.The vertical profiles of Dg and mode $\left(=D_p(n_{max})\right)$of the distributions are shown in Figure 5. It clearly shows the increase of the coarse mode fraction in the size distribution; with both the mode and Dg showing a steady increase with altitude; especially Dg. The rate of increase of Dg with altitude increases from west to east across the IGP, ~~being~~with highest values at BBR (Figure 5b). In the central IGP where mixed aerosol type prevails, the increase in Dg within the ABL is rather weak, but in the free

troposphere it increases more sharply probably due to the faster decrease in the accumulation mode concentration (Figure 4) or the prevalence of advected dust at higher altitudes or both.

The observations that have foregone reveal the non-uniform distribution of dust and anthropogenic sources of aerosols. Nearly steady values of N_C in the entire column at JDR are attributed to the strong convective mixing ~~over this region associated with intense solar heatingduring summer~~ of coarse mode dust aerosols up to the lower free tropospheric region~~whenthe surface temperatures are above 40° C (Vaishya et al., 2019)~~. On the other hand, altitude variation of accumulation and coarse mode aerosols are relatively more fluctuating at BBR and VNS, compared to that at JDR (Figure 4b) as indicated by the profiles of Dg.

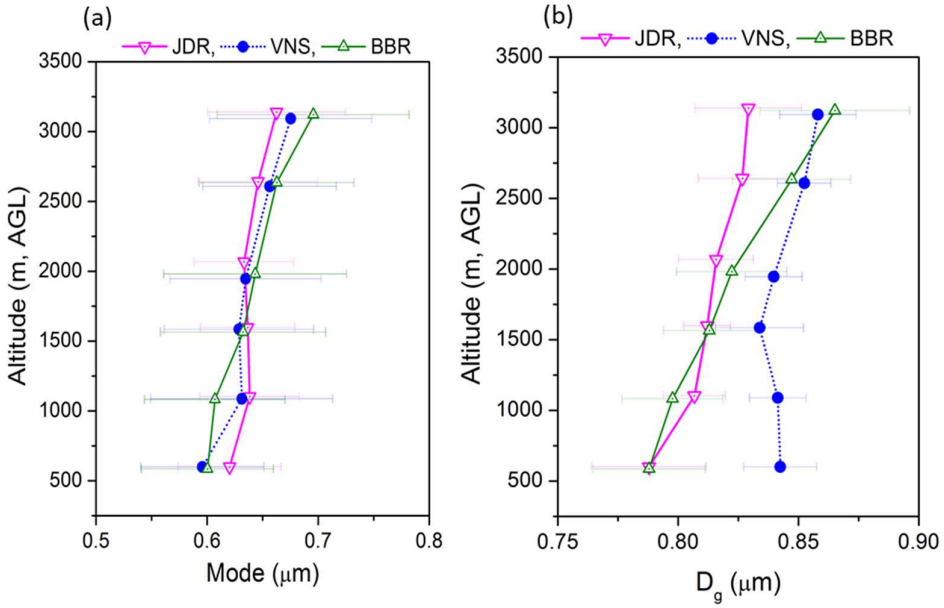

Figure-5: Vertical profiles of (a) mode and (b) geometric mean diameters (Dg) of aerosol number size distributions at different heights above the ground level, indicating the change in the pattern of distribution with altitude and from the western to the eastern part of ~~India~~the IGP.

~~These observations are also in line with the reported values of dust fractions (Vaishya et al., 2018) during the same campaign, showing the enhancement of dust fraction from 10 to 20 % at 300 m to close to 100% above 2 km altitude at JDR; while smallest dust faction (< 10%) was observed at BBR. Over the central IGP, synoptic wind driven desert dust aerosols, leads to elevated layers of aerosols having higher dust fraction (>50%). However, it should be noted that dust over the central IGP is more absorbing in nature becauseof its mixing with other anthropogenic emissions (suchas BC; Vaishya et al., 2018), while that over western IGP is rather pristine innature.Thus,~~

~~quantification of the absolute magnitude of coarse mode aerosol concentrations is very important to understand the significance of elevated aerosol load on radiative perturbations, because coarse mode dust contributes largely to aerosol scattering as well as absorption, compared to their anthropogeniccounterpart, which contributes dominantly to absorption.~~

Apart from the number-weighted expression of aerosol size distributions, the mass-weighted distributions carry useful information for quantifying regional distinctiveness of the dominance of coarse mode particles. Even though the fine mode aerosols are extremely numerous in the atmosphere and important for microphysical processes, they represent only a very small proportion of total particle mass; whereas coarse mode particles, even though far less numerous, have significant mass/ volume. In simple terms, particle number concentrations are dominant in the fine mode (< 0.1 μm), the surface area is predominantly in the accumulation mode (0.1 to 1 μm), and the volume, and hence mass, is divided between the accumulation mode and coarse particle mode. In the present study, since the size range of particle counts are confined in the accumulation and coarse mode regimes (between the 0.5 and 20μm), quantitative picture of aerosol mass concentrations is obtained by assuming a uniform density equal to 2 g cm^{-3} following Moorthy et al., (1998) and, Pillai et al., (2001). Since the size-resolved particle densities are not known, we did not use effective density (mass-mobility relationship defined as the mass of the particle divided by its mobility equivalent volume) of particles to calculate the mean particle mass size distributions.

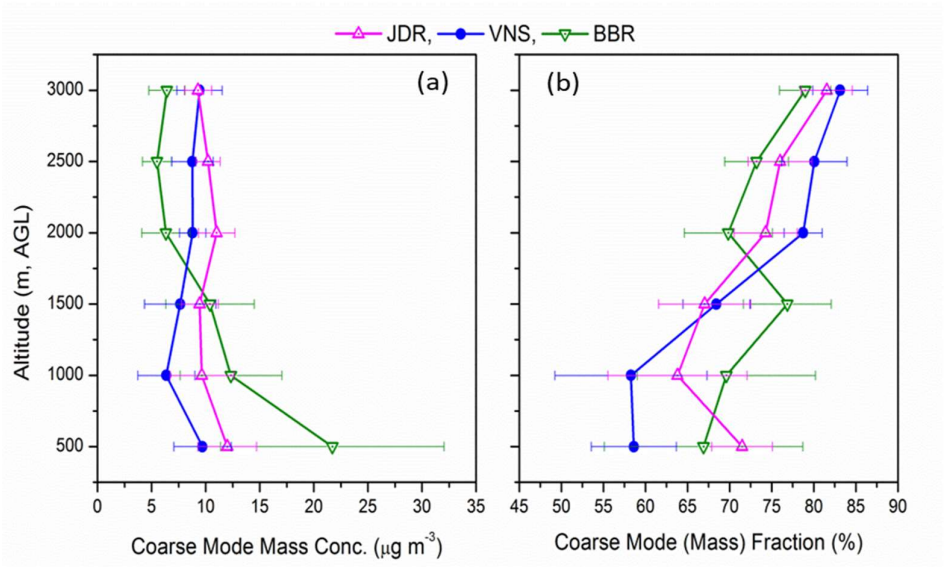

Figure-6: (a) Vertical profiles (mean and standard deviations) of coarse mode aerosol mass concentrations (M_C). The values are derived from the aerosol number concentrations at different

size bins, assuming a density of 2 gm/cm^3;(b) Vertical profiles of aerosol coarse mode fractions (F_{MC}) at different locations.

Figure 6a shows the altitudinal variation of coarse mode aerosol mass concentrations over all the observational sites, along with the values of coarse mode mass fractions (F_{MC}). Over VNS and JDR, consistently higher values of M_C were seen in the entire altitude range. This is in line with the higher values of coarse mode aerosol concentrations (N_C) at these sites, JDR being the highest. On the other hand, the values of M_C at BBR decreased significantly from the surface to lower free-tropospheric region. The higher values M_C observed near the surface at BBR can be attributed to the influence of local sea-salt aerosols; however not affecting the values of Dg, ~~as there may present~~ due to the ~~significant~~ abundance of accumulation mode aerosols over this site ~~remaining beyond the detection limit of APS~~.

Similar to that of N_C, F_{MC} showed (Figure-6b) gradually increasing values with altitude at all the locations. The high values of coarse mode mass fraction and an increasing trend with altitude is indicative of the role of upper level transport of dust from the western desert regions, in addition to those contributed locally due to thermal convective processes. As compared to other two stations, highest value of F_{MC} (~ 70%) near the surface was seen at JDR indicating the role of arid nature of the region. This exercise clearly explains the abundance coarse mode dust decreasing from west to east; along with an increase in the contribution of anthropogenic fine/ accumulation mode aerosols.

With a view to examine the ~~ing~~ transport of mineral dust (by the synoptic winds), the spatial distributions of UV-aerosol index, aerosol types and aerosol absorption optical depth (AAOD); all derived from the Level-3 OMAERUVd data product (daily, 1.0 degree x 1.0 degree) from Ozone Monitoring Instrument (OMI, on-board Aura satellite; Levelt et al., 2006), are examined. OMAERUV uses the pixel level Level-2 Aerosol data product of OMI at three wavelengths (355 nm, 388 nm and 500 nm) to derive AAOD. Higher values of AAOD at 388 nm are indicative of the presence of dust or biomass burning aerosols. ~~,~~ This is because ~~as~~ absorption by dust and organic carbon from biomass burning sources ~~are~~have strong wavelength dependency~~t~~, ~~being greater at~~ with higher absorption at ~~strong absorbers of~~ near-UV ~~radiation~~wavelengths. As the period of this campaign was devoid of major fire activities over the study region (northern India) which normally peaks in April to May and October to November, corresponding to burning after the wheat and rice harvests (Vadrevu et al., 2011; Venkataraman et al., 2006), the AAOD values would be representative of dust loading. This aspect is conformed in ~~a~~ the subsequent section using lidar depolarization ratio.

Figure 7a-d shows the spatial distributions of UV aerosol index, aerosol type and AAOD at 388 nm and 500 nm, while the synoptic winds are shown in Figure 7e. A very good association between the westerly advection and dust loading extending from west to central IGP is noticeable from the figure. This lends further support to the role of advected dust leading to higher M_C and F_{MC} at higher altitudes, seen in figures 6. In this context, it is also worth noticing that based on observational data and regional climate modeling, Banerjee et al., (2019) have clearly shown (in their Figure 7) the significant vertical extent of dust loading, both of local and remote origin, during pre-monsoon and summer across the IGP reaching altitudes as high as 600 hPa.

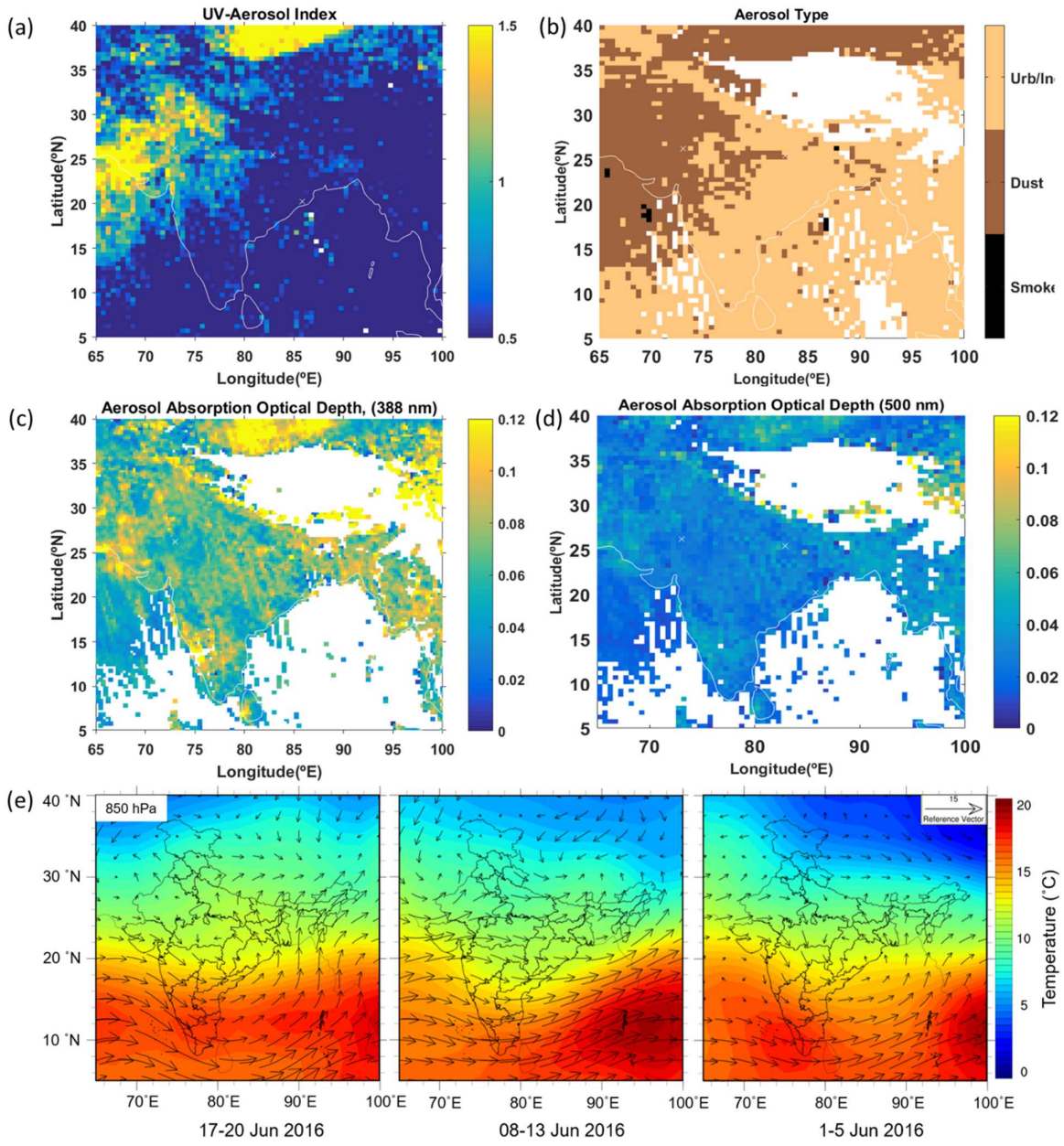

459

460 **Figure-7:** Spatial distribution of (a) UV aerosol index, (b) aerosol type, (c) aerosol absorption
461 optical depth (AAOD) at 388 nm and (d) AAOD at 500 nm during June 2016 ~~(geographic~~
462 ~~positions being shown by the 'x' marks)~~. (e) Synoptic wind and temperature at 850 hPa.

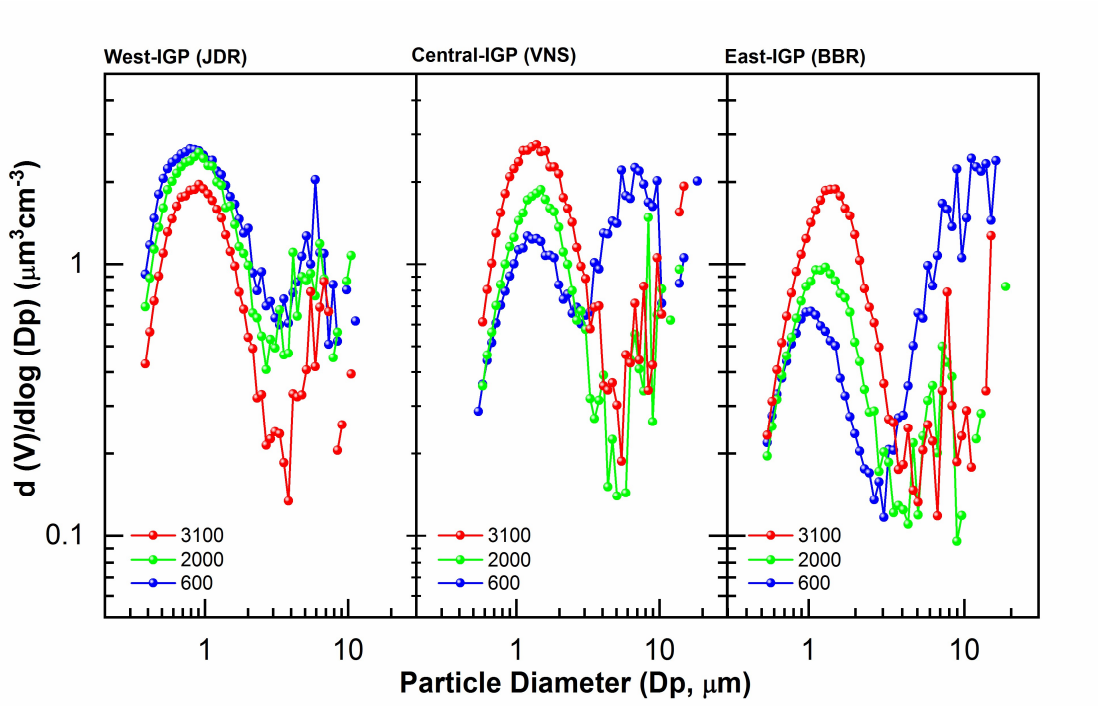

Figure-8: Aerosol volume size distributions (mean profiles averaged for all the days) at ~~distinct~~ three distinct altitudes (600 m, 2000 m and 3000 m) of the atmosphere (shown by different color) over JDR, VNS and BBR.

The volume size distribution of aerosols (shown in Figure 8) at three distinct altitude regions of the atmosphere also clearly shows the altitudinal change in the pattern of distribution, changing from coarse mode dominance near the surface to accumulation mode dominance at the ceiling altitude over BBR. While those at JDR, the pattern of distributions remains same in the entire column. Similar to JDR, VNS also depicted significant enhancement in coarse mode aerosols in the upper levels (at 2 and 3 km altitudes) of the atmosphere. Similar to these observations, based on the collocated spectral scattering properties of aerosols obtained during the same experiment, Vaishya et al., (2018) have reported that, ~~as we move from west to east in the IGP,~~ the aerosol population changes from super-micron mode dominant natural aerosols to sub-micron mode dominant anthropogenic aerosols, as we move from west to east in the IGP. Moreover, the large abundance of coarse particles (>2μm) along with significant fine/ accumulation mode aerosols in the column highlights the complex mixture of dust with other anthropogenic components in all the three regions, making a complex scenario for aerosol radiation and aerosol cloud interaction processes. Based on the combination of satellite remote sensing and regional climate model simulations, Banerjee et al., (2019) have also shown the presence of dry elevated layer of dust (at altitudes between 850 and 700 hPa; taking place in multiple layers) during June across the IGP, transported

from the Thar Desert to the northern Bay-of-Bengal. To ascertain this further, we have examined the data from CATS aboard ISS.

3.2Inferences from the CATS data

Geophysical parameters derived from the CATS on board ISS are very useful to infer on aerosol features in the atmospheric column, especially at altitudes above the ceiling altitude of the aircraft (3.1 km). In the present study, we have considered three products from CATS for the campaign period, viz. (i) depolarization ratio, (ii) attenuated backscatter coefficients and (iii) aerosol types.

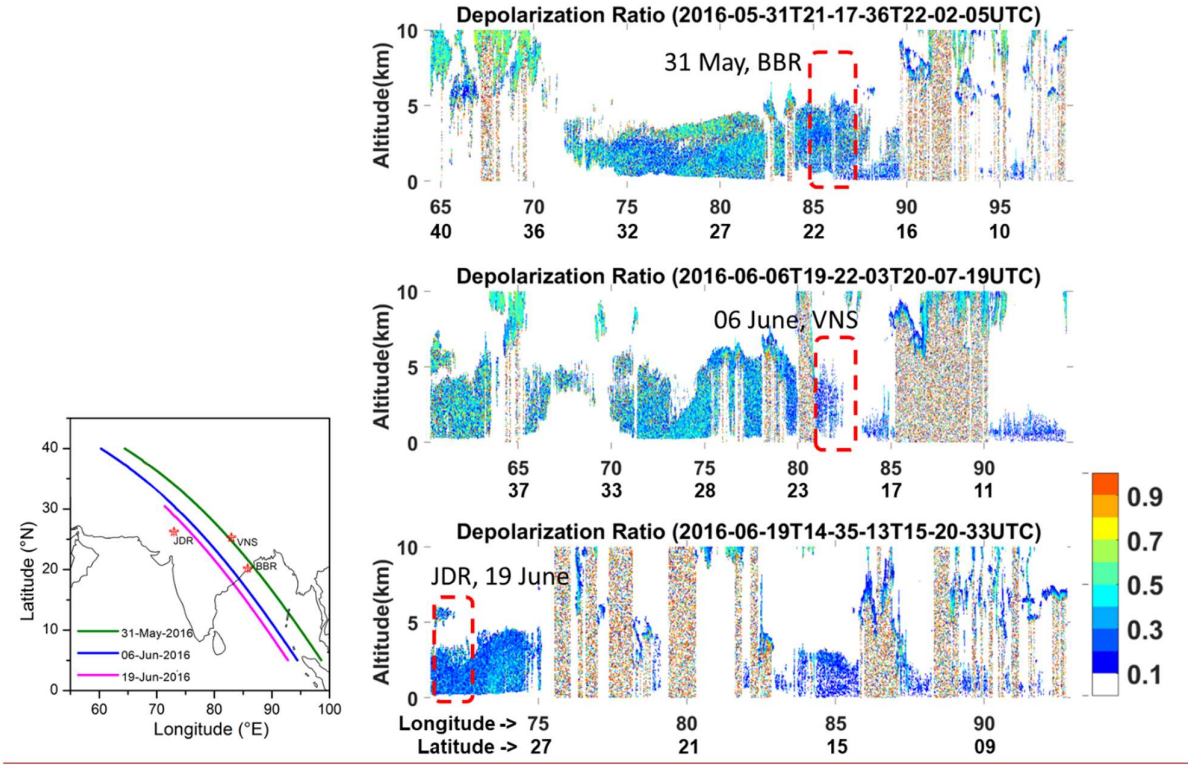

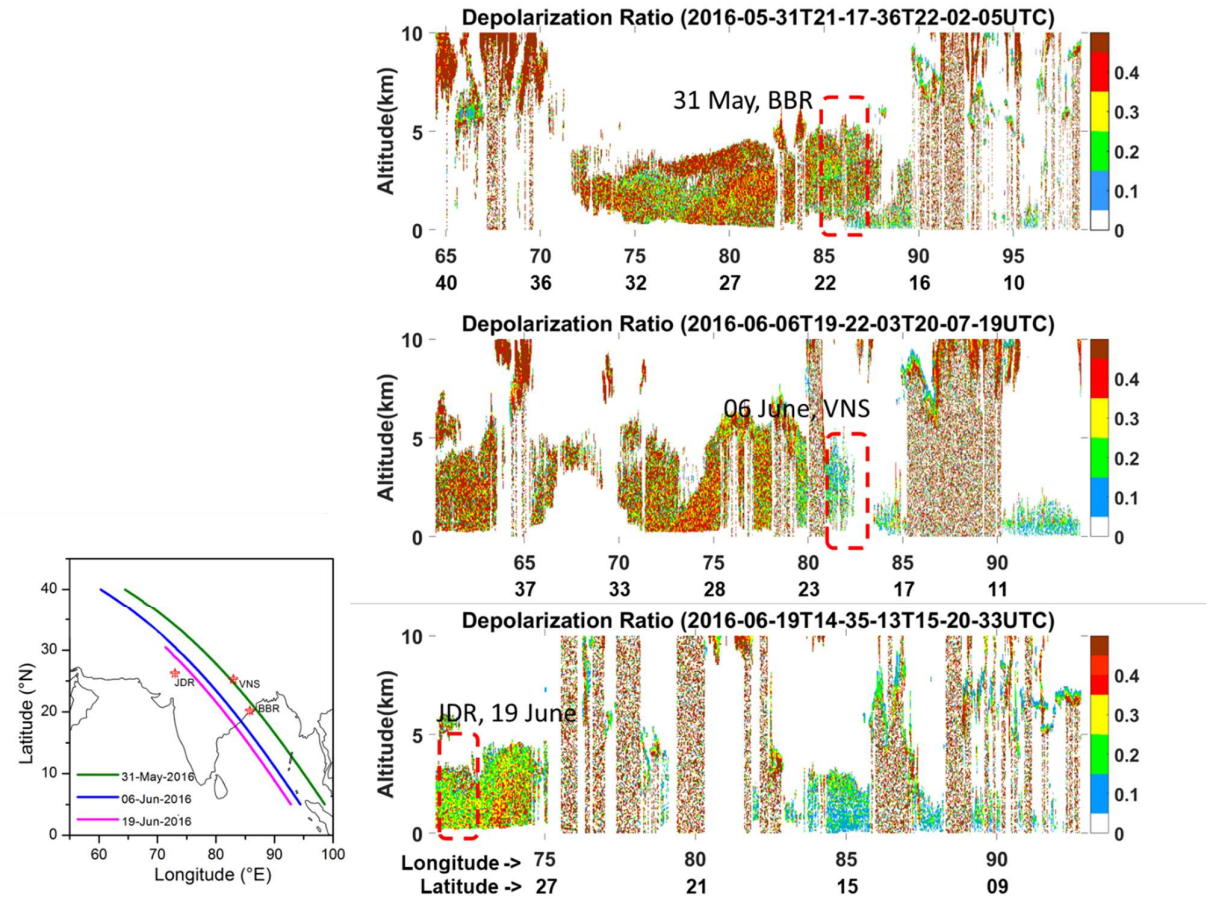

Figure-9: Aerosol Depolarization Ratio [obtained from Cloud Aerosol Transportation system in International Space Station (ISS)] for three different passes of the ISS over the three sub-regions during the period of aircraft observation. The tacks of the CATS are shown by the solid lines in the left panel and the rectangular boxes in the right panels show the data over the sub-regions.

Figure 9 shows the vertical cross-section of depolarization ratio for three passes during the campaign period and close to the three sub-regions (identified by the rectangular boxes in the figure). Higher values (~0.3) of depolarization ratios are seen in the western IGP (JDR, bottom panel), suggesting the dominance of non-spherical (dust) particles. The depolarization ratio decreases towards east across the IGP, with values ~~in the range~~ equal to 0.2~~1 and 0.3~~at the central IGP, and ~~further ~~~0.2 ~~and 0.1~~in the eastern site BBR. These lend additional support to the inference on the influence of dust aerosols during the campaign period. Supporting the patterns of depolarization ratio, aerosol types (from CATS mode 7.1) in Figure 10a indicates significant presence of dust at JDR, while the aerosol types over VNS and BBR are mixture of dust, polluted continental and carbonaceous aerosols. Vertical profiles of total attenuated backscatter coefficients

show the vertical extent of the aerosol layer to be as high as 5 km (as has been shown by Banerjee et al 2019) over all the sites (Figure 10b).

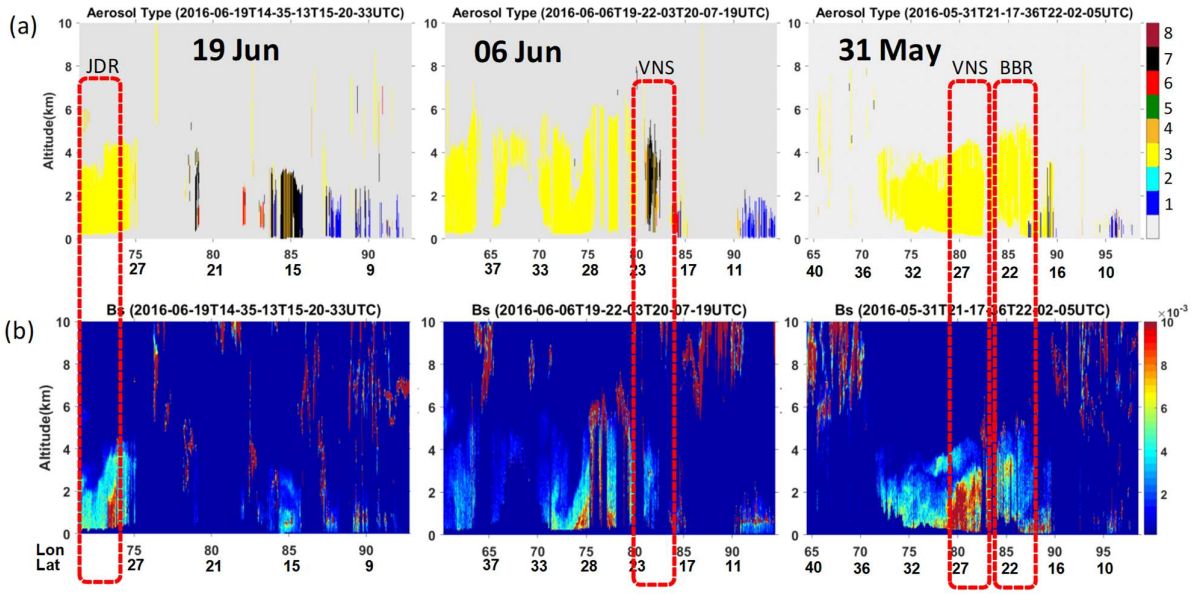

Figure-10: Transects of (a) Aerosol types (1- Marine, 2- Marine Mixture, 3- Dust, 4- Dust Mixture, 5- Clean/ Background, 6- Polluted Continental, 7- Smoke, 8- Volcanic), and (b) Backscatter coefficients (Bs, $km^{-1}Sr^{-1}$) at 1064 nm obtained during the period of aircraft observation corresponding to the overpass of the ISS.

3.3 Vertical profiles of BC

BC is the chief anthropogenic absorbing aerosol species, and the IGP is known to be among the global hotspots (Govardhan et al., 2019). The height resolved information on F_{BC} is important not only in radiative forcing, but on CCN activation as well (Bhattu et al., 2016). Collocated measurements of BC during SWAAMI - RAWEX have been used to examine the vertical profiles of BC and its variation across the IGP prior to ~~the~~ onset of the Indian summer monsoon. Figure 11a shows the vertical profiles of BC for the three sub-regions. Each profile is the average of all the profiles obtained from measurements made from each of the base station. It is seen that, BC remained low (~1 μg m^{-3}) and depicted very weak altitude variations at the western and eastern IGP regions ~~(JDR and BBR)~~, while in the central IGP ~~(VNS)~~ there is a rapid decrease of BC from the high value (~ 3μg m^{-3}) near the surface. Above 2 km, all the profiles overlap though a weak increase is indicated over BBR, which is examined later. The very high values of BC close to the

surface at VNS are attributed to the wide-spread anthropogenic activities in the Central IGP including the cluster of thermal power plants in that region. Consequently, the columnar concentration of BC (integrated up to 3 .1 km) is also the highest at VNS.

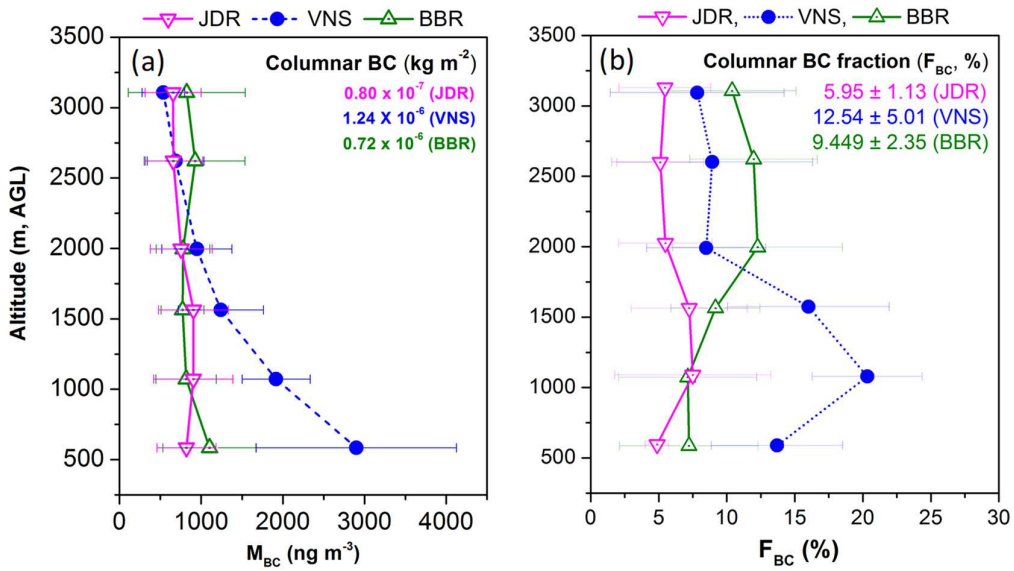

Figure-11: ~~(a)~~ Vertical profiles of ~~the~~ (a) mean values of BC mass concentrations (M_{BC}) and (b) BC mass fractions (F_{BC}) at JDR, VNS and BBR. ~~(b) Daily profiles of M_{BC} during each of the flight sorties on different days.~~

However, the vertical profiles of the fractional contribution of BC (F_{BC}) to the total composite aerosol mass (estimated from the volume size distribution, considering a uniform density of 2 gm/cc, especially in view of the abundance of dust) shows (Figure11b) sub-regional distinctiveness. It remains the lowest (~6%) in the western IGP, with very little altitude variation. In the central IGP, F_{BC} is quite high (~15 % to 20%) within the ABL and drops off fast above 2 km approaching the values seen for the western IGP. F_{BC} depicts an elevated peak at around 1 km above ground level at VNS, while at BBR, higher F_{BC} values occur at still higher altitudes at BBR, where the near-surface values are much lower and comparable to those at JDR. There is a steady increase in F_{BC} from near surface to higher altitudes, and above 2 km, the values are comparable to the peak values seen at VNS (at ~ 1 km altitude). Despite this, the integrated BC concentration comes in between those of JDR and VNS, mainly because of the large values occurring in the lower atmosphere at VNS. It may be recalled that based on SWAAMI - RAWEX aircraft measurements, Vaishya et al., (2018) have reported that while the scattering characteristics remained uniform across the IGP, the absorption coefficients showed sub-regional distinctiveness,

leading to a west to east gradient (decrease) in the vertical structure of single scattering albedo (SSA).

Investigation of the vertical profiles of BC mass concentrations on individual days (Supplementary Figure-S2) helps to see the distinctiveness at each sub-region, resulting from the spatially heterogeneous nature of emission sources and advection, especially at BBR where the inland profiles, made during sorties perpendicular to the coastline (on 2nd and 3rd June) show significantly higher values of BC at higher altitudes than those along the coastline. At BBR, this arises mainly because of spatially heterogeneous source impacts ~~that are spatially heterogeneous~~. The regions towards the northwest of BBR are characterized by large scale urban and industrial activities (Ambient air quality status and trends in Odisha: 2006 - 2014). Similarly, near surface BC concentrations at VNS was higher when the flight sorties were confined to NE, NW and SW of the city Centre, while the values in the SE sector was lower. On the other hand, at JDR, the profiles revealed a better spatial homogeneity.

~~With a view t~~To ~~o~~ quantify~~ing~~ the climatic implications of BC, the heating rate profiles of BC is examined based on the estimation of shortwave direct radiative forcing (DRF) due to BC alone. The DRF due to BC represents the difference between the DRF for aerosols with and without the BC component. The in-situ values of scattering (σ_{sca}) and absorption (σ_{abs}) coefficients measured on-board the aircraft were used to estimate spectral values of AOD (layer-integrated $\sigma_{sca}+\sigma_{abs}$), single scattering albedo (SSA) and asymmetry parameter (g) for each level, assuming a well-mixed layer of 200 m above and below the measurement altitude (details are available in Vaishya et al., 2018). The layer means values of AOD, SSA and Legendre moments of the aerosol phase function (derived from Henyey–Greenstein approximation) are used as input in the Santa Barbara DISORT Atmospheric Radiative Transfer (SBDART, Ricchiazzi et al., 1998) model to estimate diurnally averaged DRF (net flux with and without aerosols) at the top (DRF_{TOA}) and bottom (DRF_{SUR}) of each of the layers. The atmospheric forcing (DRF_{ATM}) for each of the levels is then estimated as

$$DRF_{ATM} = DRF_{TOA} - DRF_{SUR}$$

In order to estimate the forcing due to BC alone, optical parameters for aerosols were deduced again. For this, values of σ_{abs} were segregated to the contributions by BC (σ_{BC}) and OC (σ_{OC}), where σ_{BC} were estimated following inverse wavelength dependence of BC (e.g., Vaishya et al., 2017). Based on this, a new set of AOD and SSA for BC-free atmosphere is calculated and fed into SBDART for estimating DRF_{ALL-BC} without the BC component. Thus, DRF due to BC is

578 $DRF_{BC} = DRF_{ALL} - DRF_{ALL\text{-}BC}$

579 Here, DRF_{ALL} represents forcing due to all the aerosol components, including BC.

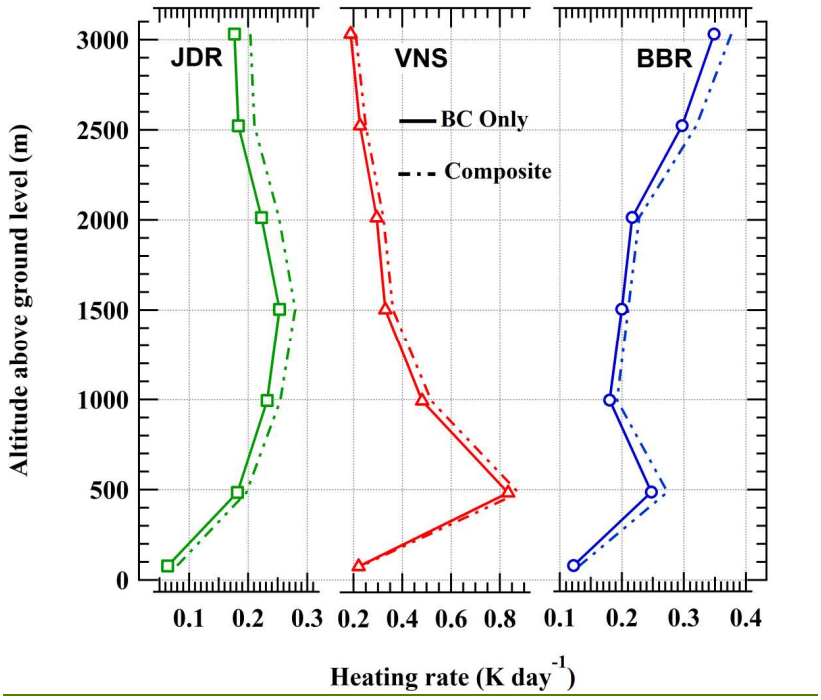

580

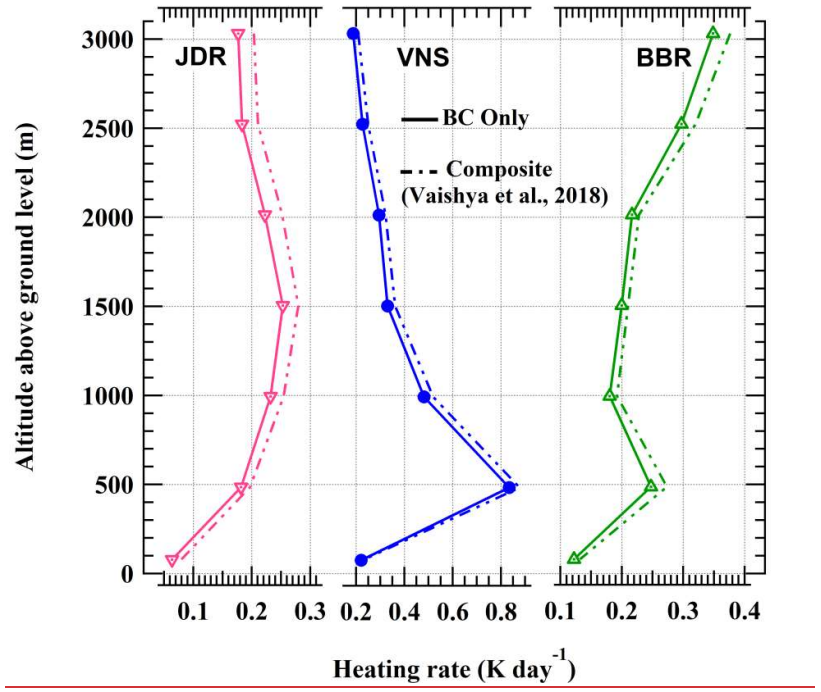

581

582 Figure-12: Vertical profiles of atmospheric heating rate due to BC (solid lines) and composite

583 (dashed lines) aerosols for the regions of the IGP: (a) JDR in western IGP, (b) VNS in central IGP

and (c) BBR in eastern IGP. Data for the composite heating rate profiles are from Vaishya et al., 2018.

The vertical profiles of atmospheric heating rate (HR, estimated based on the atmospheric pressure difference between top and bottom of each layer and aerosol induced forcing in that layer) due to BC alone shows (Figure-12) maximum influence of BC in trapping the SW-radiation at VNS, followed by BBR and JDR. Interestingly, the altitudinal profiles of heating rate are distinctly different over the regions, BBR showing an increase with altitude, while VNS shows the opposite pattern with maximum heating ~~(~~ (~ 0.81 K day^{-1}) at 500 m above ground. Enhanced heating at 500-2000 m altitude is seen at JDR. These results indicate the dominant role of absorbing aerosols near the surface at VNS, while the atmospheric perturbation due to elevated layers of absorbing aerosols is conspicuous at BBR (HR ~ 0.35 K day^{-1} at the ceiling altitude). The column integrated values of atmospheric forcing due to BC alone are 7.9 Wm^{-2}, 14.3 Wm^{-2} and 8.4 Wm^{-2} at JDR, VNS and BBR respectively.

In this context, we have examined the possible role of the large network of thermal power plants (TPP) over the northern part of India, which is reported to have a significant~~ly~~ contributione~~e~~ to regional emissions (Singh et al., 2018). These include the emissions of ~~CO~~$_2$$SO_2$, NO_{x2}, ~~S~~CO_2, CO, VOC,~~soot, CO, and~~ suspended particulate matter (~~SPM~~PM2.5 and PM10, including BC and OC) and other trace ~~gas species~~metals like mercury (Guttikanda and Jawahar, 2014; Sahu et al., 2017), dispersing over large areas through stacks. Fly ash from coal-fired power plants cause severe environmental degradation in the nearby environments (5-10 km) of TPP (Tiwari et al., 2019). Over the IGP, since ~~M~~more than 70% of the thermal power plants ~~over the IGP~~ are coal based, emissions of ~~and~~ CO_2 and SO_2 hold more than 47% of the total emission share, while the relative share of PM2.5 and NOx are ~15% and 30% (GAINS, 2012). Based on the in-situ measurement of BC in fixed and transit areas in close proximity of seven coal-fired TPP in Singrauli (located ~ 700 km north-west of BBR), Singh et al., (2018) have reported that BC concentration reached as high as 200 µg $m^{-}3$ in the transit measurements. The E~~e~~nergy and R~~r~~esources I~~i~~nstitute, India have also reported that emission levels of the carbonaceous (soot or BC) particles are estimated to be around 0.061 gm/kWh per unit of electricity from Indian thermal power plants (Vipradas et al., 2004). Based on emission pathways and ambient PM2.5 pollution over India, Venkataraman et al., (2018) have reported that the types of aerosols emitted from coal burning in thermal power plants and industry in eastern and peninsular India are similar to that of residential biomass combustion. The ongoing discussion thus clearly indicates that TPP are major sources of BC in the atmosphere.

As it is not possible to measure ~~soot~~BC from space, to infer on the role of these emissions from thermal power plants in causing the higher BC fraction at higher a~~t~~ltitude over BBR, we have examined the spatial distribution of the concentrations of the co-emitted NO_2 and SO_2 in Figure 13~~12~~,in which the locations of major coal based ~~thermal power plants (~~TPP (https://www.ntpc.co.in/en/power-generation/coal-based-power-stations) are also marked. The data are obtained from OMI onboard AURA satellite. Higher concentrations of NO_2 and SO_2 are readily discernible from the figure around the regions (marked in the figure) during the period of flight experiment where there are clusters of ~~thermal power plants~~TPP. As the energy consumption is the highest during summer and most dependent on thermal, these TPP should be operating to near full capacity. This provides an indirect support to the high concentrations of BC (co-emitted) at higher levels. ~~Similar~~ In general, these TPP~~s~~ have tall stacks (heights in the range 200 to 400 m) and aids easy ventilation to the lower free-tropospheric altitudes.

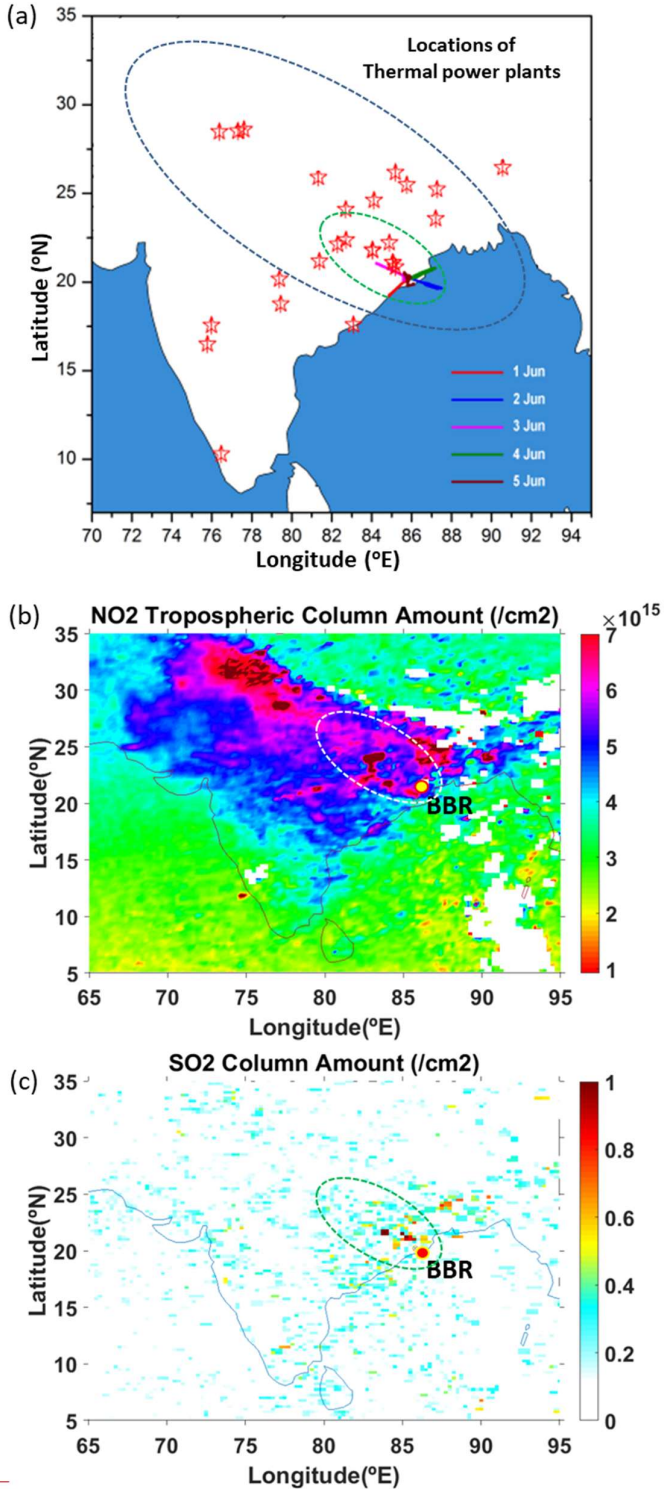
(a)
Locations of
Thermal power plants
1 Jun
2 Jun
3 Jun
4 Jun
5 Jun
Latitude (°N)
Longitude (°E)
(b)
NO2 Tropospheric Column Amount (/cm2)
×10^15
BBR
Latitude(°N)
Longitude(°E)
(c)
SO2 Column Amount (/cm2)
BBR
Latitude(°N)
Longitude(°E)

628

629

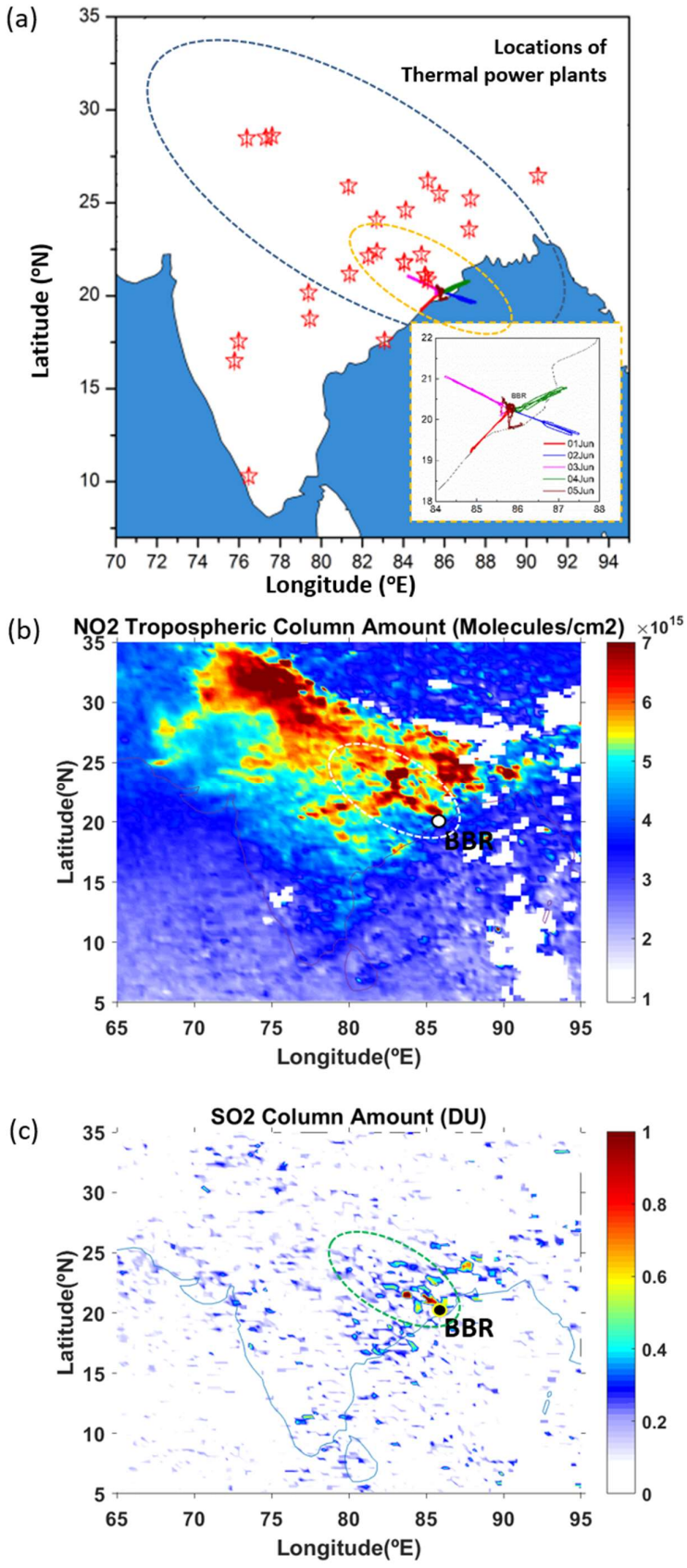
(a)
Locations of
Thermal power plants
Latitude (°N)
Longitude (°E)
BBR
01Jun
02Jun
03Jun
04Jun
05Jun
(b)
NO2 Tropospheric Column Amount (Molecules/cm2)
×10^15
Latitude(°N)
Longitude(°E)
BBR
(c)
SO2 Column Amount (DU)
Latitude(°N)
Longitude(°E)
BBR

630

Figure-~~12~~13: (a) Geographic position of thermal power plants (TPP) over India (the TPP across the IGP are bounded by the blue dashed line, and those along the flight direction of BBR are bounded by the green dashed line), along with the spatial map of ~~tropospheric column abundance of (b) SO_2 column amount (DU) and~~ (~~b~~e) NO_2 tropospheric column density (molecules/cm^2) ~~over the northern part of India~~and (c) SO_2 column amount (in DU, 1DU = 2.69 x 10^{16} molecules/cm^2) over the northern part of India.~~.~~

To further ascertain this, the spectral properties of aerosol absorption are examined. First, we have examined the frequency distribution of absorption Ångström ~~absorption~~ exponent (α_{abs}, derived from the linear fit on log-log scale between corresponding absorption coefficients to aethalometer wavelengths)in Figure ~~13~~14; separately for the mixed layer (ML, below 1.5 km) and above (≥2km). The frequency distribution of α_{abs} reveals a clear shift towards lower values as we move from JDR to BBR, both within the ML and above, even though the values of α_{abs} lying mostly between 1 and 1.5. Based on laboratory studies and field investigations, it has ~~already~~ been shown that the higher values of α_{abs} (~ 2) are representative of biomass burning emissions, while the values ~ 1 are indicative of fossil fuel combustions (Kirchstetter et al., 2004). The values of α_{abs}>1 is indicative of the presence of biomass-burning, whose relative abundance increase with the steepness of the absorption spectra, as has been reported elsewhere from the laboratory experiments (~~[~~Hopkins et al., 2007)~~]~~.

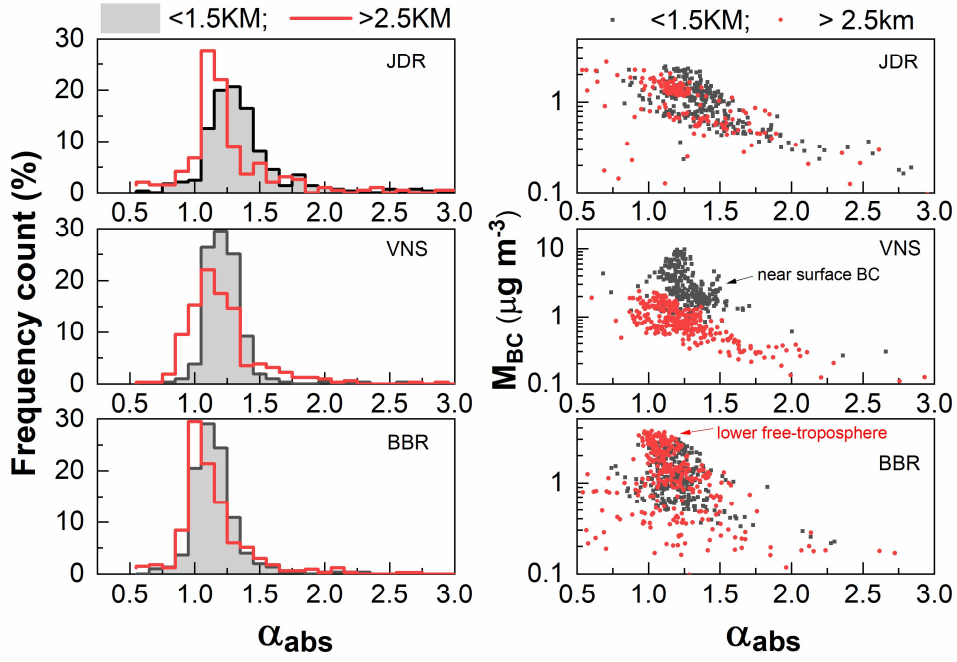

Figure-~~13~~14: (a) Frequency of occurrences of Angstrom absorption exponent (α_{abs}) below 1.5 km and above 2.5 km altitude, (b) variation of BC mass concentrations corresponding to different values of α_{abs} are shown in the right panels for the same two altitude regimes at distinct locations of northern India.

Examining Figure ~~13~~ 14 in the above light, it emerges that significant contribution of BC ~~of~~ from fossil fuel combustions mixed with biomass burning origin prevails at higher altitudes over BBR, while the association between the two decreases abruptly from ML to higher height at VNS. The consistent higher values of BC in the column associated with the values of α_{abs} lying between 1 and 1.5 ~~are indicative of influence of anthropogenic sources at BBR. This~~ can also be due to the aging of BC at higher heights, during which BC mixes with other species and its angstrom exponent increases, as the spectral dependence of absorption steepens when BC (even though its source could be fossil fuel) is coated with a concentric shell of weakly absorbing material (Gogoi et al., 2017). Further investigations are needed in this direction.

3.4 Inter-seasonal variability: a case study at JDR~~Finds from the present study Vs results reported for other seasons~~

The spatial variation of the altitude profiles of N_{AC}, Dg, F_{MC} and F_{BC} across the IGP hints to several possible implications of their direct and indirect effects. Altitudinal increases in the values of Dg and F_{MC} along with depolarization ratios are indicative of the presence of dust (> 4 μm) in the lower free troposphere, which is known to produce long-wave (warming) radiative effect (Miller et al., 2006; Tegen and Lacis, 1996). Conversely, significant abundance of accumulation mode aerosols, in general, might contribute significantly to scattering. ~~Based on air-borne measurements during SWAAMI – RAWEX, Vaishya et al., (2018) have reported that the values of SSA varied between 0.935 (at 550) in spring to 0.84 (at 530 nm) during pre-monsoon period, indicating a seasonal change in the aerosol type and consequently their optical properties.~~ For example, a clear seasonal change in the vertical profiles of N_{AC} is noticeable at JDR, changing of the much steeper variation (vertically) in winter (as reported by Gogoi et al., 2019) to a near-steady one during just prior to the onset of monsoon (Figure ~~14~~15). Based on air-borne measurements during SWAAMI - RAWEX, Vaishya et al., (2018) have reported that the values of SSA at west IGP varied between 0.935 (at 530) in spring to 0.84 (at 530 nm) during prior to onset of monsoon, indicating a seasonal change in the aerosol type and consequently their optical properties.

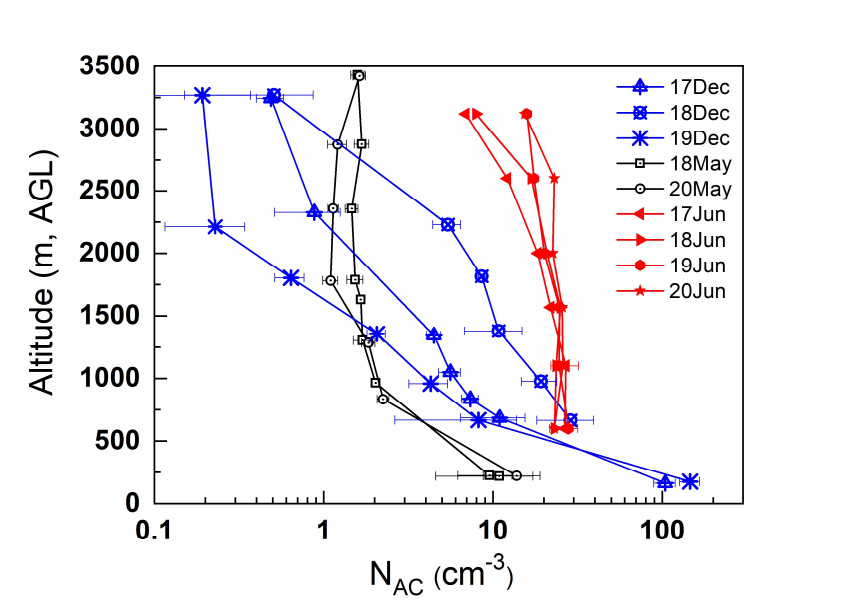

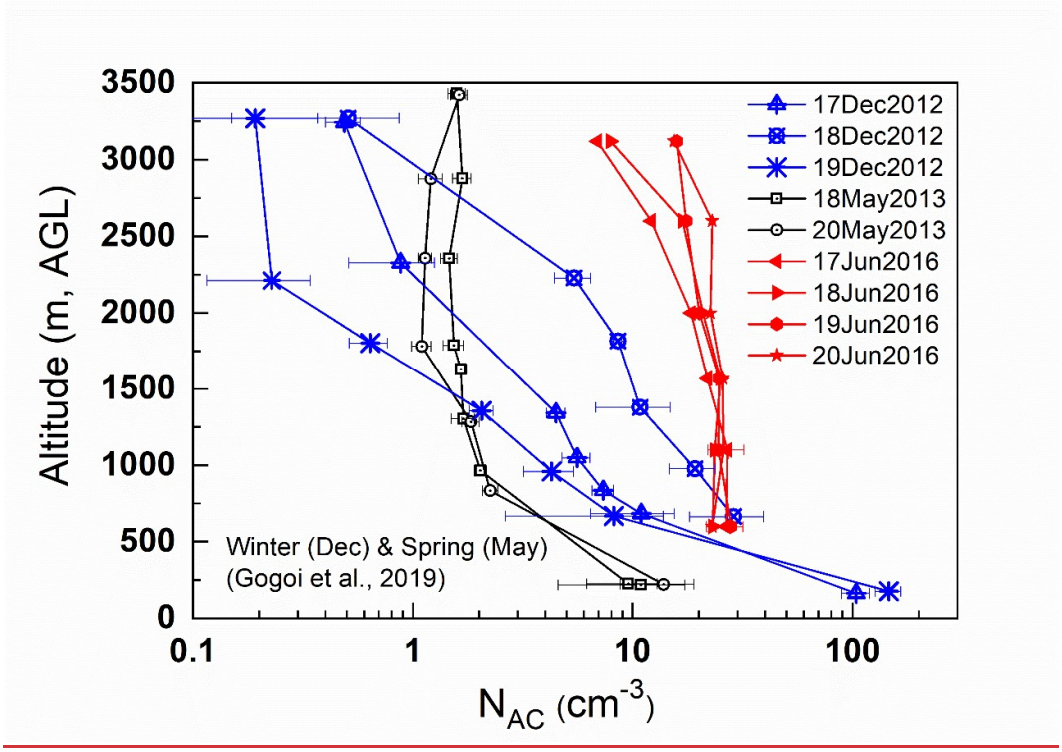

Figure-~~14~~15: Vertical profiles of seasonal mean values of aerosol accumulation and coarse mode number concentrations (N_{AC}) at Jodhpur during winter-2012 (17-19 Dec), spring-2013 (~~19~~ 18 and 20 May) and just prior to the onset of monsoon-2016 (17-20 June).

To examine the role of the ~~changing synoptic meteorology~~dynamical processes ~~during this period~~at different seasons, we have shown the profiles of vertical velocity (in pressure coordinates from 1000 hPa to 100 hPa) in Figure ~~15~~16. These are obtained from ERA-interim reanalysis data

sets. Here, the positive and negative signs of vertical velocity (ω) are indicative of updraft (as indicated by -ve values of ω) and downdraft (as indicated by +ve values of ω). A clear seasonal transformation is seen, with increasingly stronger updrafts dominating over the IGP from December to June, with the intensity increasing from west to east. In the western IGP regions, the sign of vertical velocity is seemed to change from December to June, progressively enhancing the magnitude of deep convection towards the onset of monsoon imparting stronger vertical dispersion and more homogeneous distribution of aerosols in the column.

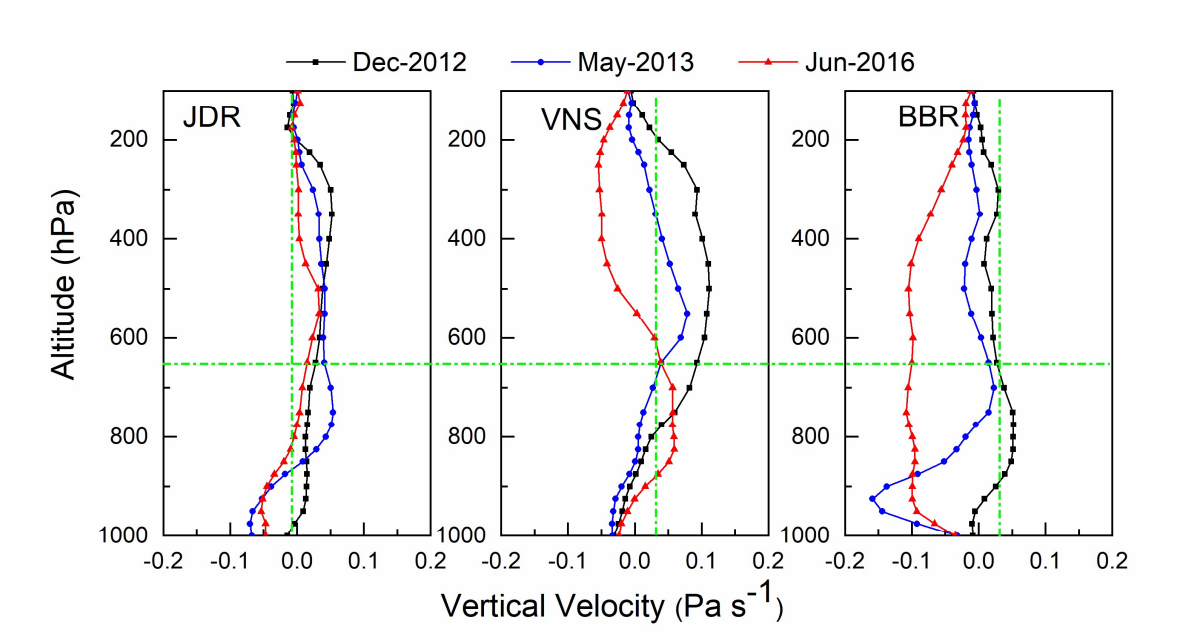

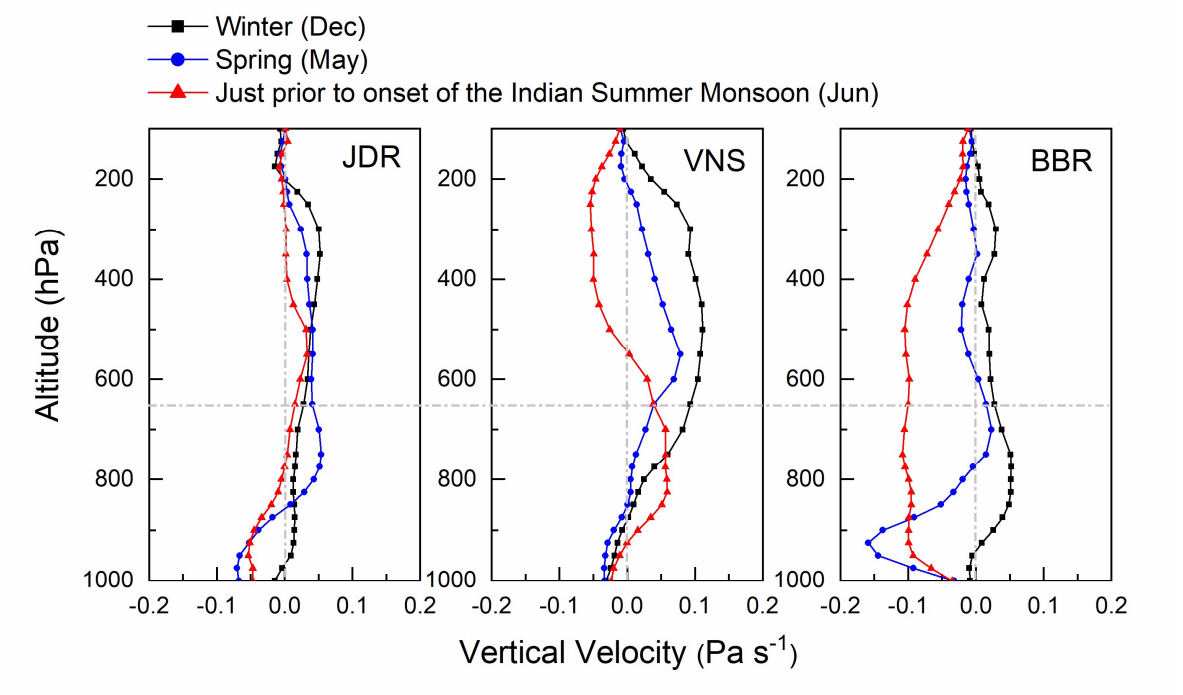

Figure ~~15~~16: Vertical profiles of vertical velocity (Pa s^{-1}) over the study locations representing Winter (December, 2012), Spring (May, 2013) and ~~summer,~~ just prior to ~~the~~ onset of the Indian Summer Monsoon (June, 2016) at different pressure levels from 1000 to 100 hPa. The positive and negative values are indicative of the descending and ascending motions respectively. The horizontal dashed line indicated the ceiling altitude (~ 3.5 km above ground level) of aircraft measurements while the vertical dashed lines mark the boundary of vertical velocity (= 0) changing from positive to negative and vice versa.

Regionally, the seasonal transformation of vertical velocity ~~The above feature~~ is more prominent over the eastern IGP -'BBR', where the magnitude of vertical velocity is consistently higher from surface to upper tropospheric regions prior to the onset of monsoon~~supporting deep convection~~. During this period, ~~T~~the head -Bay of Bengal is known to be one of the regions where deep convection exists ~~prior to the onset of monsoon~~ (Bhat et al., 2001). Since size distribution is a dominant factor in determining the direct radiative forcing (Tegen and Lacis, 1996; Liao and Seinfeld, 1998; Seinfeld et al., 2016), a clear seasonal change in the altitudinal variations of aerosol type and size distributions associated with distinct transport and convective processes will have strong radiative impact. Especially the columnar distribution of coarse mode dust and highly absorbing BC need explicit representations in climate models for accurate understanding of the net TOA direct radiative forcing. Apart from the direct radiative implications, abundance of coarse mode dust particles (having sizes larger than critical diameter) and aged BC (coated with hygroscopic materials) in the lower free troposphere can act as cloud condensation nuclei (CCN) in a supersaturated environment. Recent studies suggest that mineral aerosols are the dominant ice nuclei for cirrus clouds (Storelvmo and Herger, 2014).

4. Summary and Conclusions

Extensive air-borne measurements of aerosol number-size distribution profiles are carried out, for the first time across the IGP prior to the onset of Indian summer monsoon as part of SWAAMI - RAWEX. Collocated measurements of BC profiles are also carried out. The main findings are:

- Aerosol size distribution depicted significant altitudinal variation in the coarse mode regime, at western IGP (represented by JDR), having highest coarse mode mass fraction (72%) near the surface; while BC mass fractions (F_{BC}) as well as aerosol accumulation and coarse mode number concentrations (N_{AC}) remained nearly steady from surface to the ceiling altitude (~ 3.5 km) of the aircraft measurements. However, the pattern was significantly different at eastern IGP (represented by BBR) transforming to gradually

decreasing values of coarse mode mass concentration (M_C) and N_{AC}, but with a corresponding increase in the values of F_{BC} with altitude. At sub-regional scales, BBR depicted higher spatial heterogeneity in the above aerosol characteristics; while highest homogeneity was observed at JDR.

- Number concentrations showed dominance of accumulation mode near the surface, with the Central IGP station Varanasi (VNS) depicting the highest values N_{AC} (~~and (~~F_{BC} ~ 15%), while the coarse mode remained nearly steady throughout the vertical column.

- Atmospheric heating rate due to BC is highest near the surface at VNS (~ 0.81 K day^{-1}), while showing an increasing pattern with altitude at BBR (~ 0.35 K day^{-1}) at the ceiling altitude.

- Our measurements, supplemented with information from different space-borne sensors (CATS aboard ISS; OMI) and model results clearly indicated role of mineral dust; both locally generated and advected from the west Asian region, in contributing to the aerosol loading across the IGP, especially at free-tropospheric altitudes. The vertical extents of these layers reached as high as 5 km during the period of observation.

- ~~Thermal power plants are important contributors to higher BC fraction at higher altitude over the eastern part (BBR), while local anthropogenic sources are more prominent near the surface at central IGP (VNS).~~

Data availability

Details of aircraft data used in this manuscript and the point of contact are available at http://spl.gov.in; "Research Themes"; "Aerosols and Radiative Forcing".

Authors contributions

SSB, SKS and KKM conceptualized the experiment and finalized the methodology. SSB, MMG, VJ and AV conducted the measurement on board aircraft. MMG carried out the scientific analysis of the aircraft data and drafted the manuscript with contributions from AV and VJ. KKM, SKS and SSB carried out the review and editing of the manuscript.

Competing interests

The authors declare that they have no conflict of interest.

Acknowledgement

This study was a part of joint Indo-UK field campaign, South-West Asian Aerosol Monsoon Interactions ~~(SWAAMI) carried out jointly with~~ - Regional Aerosol Warming Experiment (SWAAMI - RAWEX). The aircraft and the flying support were provided by National Remote Sensing Centre (NRSC), Hyderabad. SKS would like to acknowledge J.C. Bose Fellowship awarded to him by SERB-DST. AV was supported by the Department of Science and Technology, Government of India through its INSPIRE Faculty programme. We acknowledge the CATS science team for providing valuable data sets (freely) for scientific applications. The RAWEX project is supported by ISRO (Indian Space Research Organisation) and the SWAAMI project is supported by MoES (Ministry of Earth Science), Government of India. ~~The in-situ data used in the present study is made available at http://spl.gov.in/RAWEX.~~[SSB1][SSB2]

References

Ambient air quality status and trends in Odisha: 2006 – 2014: Published by State Pollution Control Board, Odisha, 2015.

Arnott, W. P., Hamasha, K., Moosmuller, H., Sheridan, P.J. and Ohren, J.A.: Towards aerosol light-absorption measurements with a 7-wavelength aethalometer: Evaluation with a photoacoustic instrument and 3-wavelength nephelometer. Aerosols Sci. Technol., 39(1), 17-29, 2005.

Babu, S.S., Nair, V.S., Gogoi, M.M. and Moorthy, K.K.: Seasonal variation of vertical distribution of aerosol single scattering albedo over Indian sub-continent: RAWEX aircraft observations. Atmos. Environ., 125, 312–323, https://doi.org/10.1016/ j.atmosenv.2015.09.041, 2016.

784 Banerjee, P., Satheesh, S.K., Moorthy, K.K., Nanjudiah, R.S., Nair, V.S.: Long-Range Transport
785 of Mineral Dust to the Northeast Indian Ocean: Regional versus Remote Sources and the
786 Implications, J. Climate, 32, 1525-1549, DOI: 10.1175/JCLI-D-18-0403.1, 2019.

787 Bansal, O., Singh, A., Singh, D.: Aerosol Characteristics over the Northwestern Indo-Gangetic
788 Plain: Clear-Sky Radiative Forcing of Composite and Black Carbon Aerosol, Aerosol Air
789 Quality Res., 19: 5–14, 2019.

790 Bhat, G.S., Gadgil, S., Kumar, P.V.S., Kalsi, S.R., Madhusoodanan, P., Murty, V.S.N., Rao,
791 V.V.K.P., Babu, V.R., Rao, L.V.G., Rao, R.R., Ravichandran, R., Reddy, K.G., Rao, P.S.,
792 Sengupta, D., Sikka, D.R., Swain, J. and Vinayachandran, P.N.: BOBMEX: The Bay of
793 Bengal Monsoon Experiment, Bull. American Met. Society. 82, 10, 2217-2243, 2001.

794 Bhattu, D., Tripathi, S., Chakraborty, A.: Deriving aerosol hygroscopic mixing state from size-
795 resolved ccn activity and HR-TOF-AMS measurements, Atmos. Environ., 142, 57-70, 2016.

796 Brooks, J., James D.A., Paul I. et al.: Vertical and horizontal distribution of submicron aerosol
797 chemical composition and physical characteristics across northern India during pre-monsoon
798 and monsoon seasons. Atmos. Chem. Phys. 19, 5615–5634, 2019.

799 Corrigan, C.E., Ramanathan, V. and Schauer, J.J.: Impact of monsoon transitions on the physical
800 and optical properties of aerosols. J. Geophys. Res., 111, D18208,
801 doi:10.1029/2005JD006370, 2006.

802 Gautam, R., Hsu, N.C. and Lau, K.M.: Premonsoon aerosol characterization and radiative effects
803 over theIndo-Gangetic Plains: Implications for regional climate warming, J. Geophys. Res.,
804 115, D17208, doi:10.1029/2010JD013819, 2010.

805 Gautam, R., Hsu, N.C., Tsay, S.C., Lau, K.M., Holben, B., Bell, S. et al.: Accumulation of aerosols
806 over the Indo-Gangetic plains and southern slopes of the Himalayas: distribution, properties
807 and radiative effects during the 2009 pre-monsoon season. Atmos. Chem. Phys. 11, 12841–
808 12863, 2011.

809 Giles, D. M., Holben, B. N., Eck, T. F., Sinyuk, A., Smirnov, A., Slutsker, I., Dickerson, R. R.,
810 Thompson, A. M. and Schafer, J. S.: An analysis of AERONET aerosol absorption
811 properties and classifications representative of aerosol source regions, J. Geophys. Res., 117,
812 D17203, doi:10.1029/2012JD018127, 2012.

813 Gogoi, M.M., Babu, S.S., Moorthy, K.K., Bhuyan, P.K., Pathak, B., Subba, T., Chutia, L., Kundu,
814 S.S., Bharali, C., Borgohain, A., Guha, A., De, B.K., Singh, B., and Chin, M.: Radiative

effects of absorbing aerosols over northeastern India: Observations and model simulations. J. Geophys. Res., 122, doi:10.1002/2016JD025592, 2017.

Gogoi, M.M., Lakshmi, N.B., Nair, V.S., Kompalli, S.K., Moorthy, K.K. and Babu, S.S., 2019. Seasonal contrast in the vertical profiles of aerosol number concentrations and size distributions over India: implications from RAWEX aircraft campaign. J. Earth Sys. Sc., 128 225, DOI: 10.1007/s12040-019-1246-y, 2019.

Govardhan, G., Satheesh, S.K., Moorthy, K.K. and Nanjundiah, R.: Simulations of Black Carbon Over Indian Region: Improvements and implications of diurnality in emissions Atmos. Chem. Phys. ~~Discuss~~., 20, 561–576, doi:10.5194/acp-20-561-2020, 2020. ~~https://doi.org/10.5194/acp-2019-152, 2019~~.

Jayachandran, V.N., Babu, S.S., Vaishya, V., Gogoi, M.M., Nair, V.S., Satheesh, S.K., Moorthy, K.K.: Altitude profiles of cloud condensation nuclei characteristics across the Indo-Gangetic Plain prior to the onset of the Indian summer monsoon, Atmos. Chem. Phys., 20, 561–576~~,~~ ~~2020~~, doi:10.5194/acp-20-561-2020, 2020

Kedia, S., Ramachandran, S., Holben, B.N., Tripathi, S.N.: Quantification of aerosol type, and sources of aerosols over the Indo-Gangetic Plain. Atmos. Env., 98, 607-619, 2014.

Kirchstetter, T. W., Novakov, T. and Hobbs, P. V.: Evidence that the spectral dependence of light absorption byaerosols is affected by organic carbon,J.Geophys. Res.,109, D21208, doi:10.1029/2004JD004999, 2004.

~~Konwar, M., Panicker, A.S., Axisa, D. and Prabha, T.V.: Near cloud aerosols in monsoon environment and its impact on radiative forcing. J. Geophys. Res., doi: 10.1002/2014JD022420, 2015.~~

Kulkarni, J. R., Maheskumar, R. S., Morwal S. B; Padma Kumari B., Konwar M., Deshpande C. G., Joshi R. R., Bhalwankar R. V., Pandithurai G., Safai P.D., Narkhedkar S. G., Dani K. K., Nath A., Nair Sathy, Sapre V. V., Puranik P. V., Kandalgaonkar S., Mujumdar V. R., Khaladkar R. M., Vijayakumar R., Prabha T. V. and Goswami B. N.: The Cloud Aerosol Interactions and Precipitation Enhancement Experiment (CAIPEEX): Overview and Preliminary Results, Current Science, 102(3), 413-425, 2012.

Kumar, M., Parmar, K.S., Kumar, D.B., Mhawish, A., Broday, D.M., Malla, R.K., Banerjeea, T.: Long-term aerosol climatology over Indo-Gangetic Plain: Trend, prediction and potential source fields. Atmos. Env., 180, 37–50, 2018.

Lee et al.: Investigation of CATS aerosol products and application toward global diurnal variation of aerosols, Atmos. Chem. Phys. Discuss., https://doi.org/10.5194/acp-2018-1298 2019.

Levelt, P. F., van den Oord, G. H. J., Dobber, M. R., Mälkki, A., Visser, H., de Vries, J., Stammes, P., Lundell, J. O. V., and Saari, H.: The Ozone Monitoring Instrument, IEEE Trans. Geosci. Remote Sens., 44, 1093–1101, doi:10.1109/TGRS.2006.872333, 2006.

Li, Z., et al.:Aerosol and monsoon climate interactions over Asia, Aerosol and monsoon climate interactions over Asia, Rev. Geophys., 54, 866–929, doi:10.1002/2015RG000500, 2016.

Liao, H. and Seinfeld, J.H.: Radiative forcing by mineral dust aerosols: Sensitivity to key variables. J. Geophys. Res., 103, 31,637–31, 645, 1998.

Mhawish, A., Banerjeea, T., Broday, D.M., Misra, A., Tripathi, S.N.: Evaluation of MODIS Collection 6 aerosol retrieval algorithms over IndoGangetic Plain: Implications of aerosols types and mass loading, Remote Sens. Env., 201, 297–313, 2017.

Miller, R. L. et al.: Mineral dust aerosols in the NASA Goddard Institute for Space Sciences ModelE atmospheric general circulation model. J. Geophys. Res. 111, D06208, doi:10.1029/2005JD005796, 2006.

Mitchell, J.P. and Nagel, M.W., Time-of-flight aerodynamic particle size analysers: their use and limitations for the evaluation of medical aerosols, J. Aerosol. Medicine, 12, 4, 217-240, 1999.

Moorthy, K. K., Babu, S.S., Satheesh, S.K., Srinivasan, J. and Dutt, C.B.S.: Dust absorption over the ‘‘Great Indian Desert’’ inferred using ground-based and satellite remote sensing, J. Geophys. Res., 112, D09206, doi:10.1029/2006JD007690, 2007.

Moorthy, K.K., Babu, S.S., Satheesh, S.K., Srinivasan, J. and Dutt, C.B.S.: Dust absorption over the ‘‘Great Indian Desert’’ inferred using ground-based and satellite remote sensing. J. Geophys. Res., 112, D09206, doi:10.1029/2006JD007690, 2007.

Moorthy, K.K., Satheesh, S.K. and Kotamarthi, V.R., Evolution of aerosol research in India and the RAWEX–GVAX: an overview, Current Sc., 111, 1, 2016.

Moorthy, K.K., Satheesh, S.K., Murthy, B.V.K.: Characteristics of spectral optical depths and size distributions of aerosols over tropical oceanic regions, J. Atmos. Sol. Terr. Phys., 60, 981-992, 1998.

Nair, V. S., Babu, S.S., Gogoi, M.M. and Moorthy, K.K.: Large-scale enhancement in aerosol absorption in the lower free troposphere over continental India during spring, Geophys. Res. Lett., 43, 11,453–11,461, doi:10.1002/2016GL070669, 2016.

878 Nath, R., Luo, Y., Chen, W. and Cui, X.: On the contribution of internal variability and external
879 forcing factors to the Cooling trend over the Humid Subtropical Indo-Gangetic Plain in
880 India. Sci. Reports., 8:18047, DOI:10.1038/s41598-018-36311-5, 2018.
881 Padmakumari, B., Maheskumar, R.S., Harikishan, G., Morwal, S.B., Prabha, T.V., Kulkarni, J.R.:
882 In situ measurements of aerosol vertical and spatial distributions over continental India
883 during the major drought year 2009, Atmos. Env., 80, 107-121, 2013.
884 Panda, U., Das, T.: Micro-structural analysis of individual aerosol coarse particles during different
885 seasons at an eastern coastal site in India. Atmos. Pollution Res., DOI:
886 10.1016/j.apr.2016.08.012, 2016.
887 Pandey, S.K., Vinoj, V., Landu, K. and Babu, S.S.: Declining pre-monsoon dust loading over
888 South Asia: Signature of a changing regional climate. Sci. Reports., 7:16062,
889 DOI:10.1038/s41598-017-16338-w, 2017.
890 Pillai, P. S., and Moorthy, K.K.: Aerosol mass-size distributions at a tropical coastal environment:
891 Response to mesoscale and synoptic processes, Atmos. Environ., 35, 4099– 4112, 2001.
892 Praveen, P.S., Ahmed, T., Kar, A., Rehman, I.H. and Ramanathan, V.: Link between local scale
893 BC emissions in the Indo-Gangetic Plains and large scale atmospheric solar absorption,
894 Atmos. Chem. Phys., 12, 1173–1187, 2012.
895 Rana, A., Jia, S., Sarkar, S.: Black carbon aerosol in India: A comprehensive review of current
896 status and future prospects. Atmos. Res., 218, 207–230, 2019.
897 Seinfeld, J.H. et al., 2016. Improving our fundamental understanding of the role of aerosol-cloud
898 interactions in the climate system. Proc. Natl. Acad. Sci. U S A. 113(21): 5781–5790.
899 Singh, A., Khadak S.M., Ruphaketi, M., Junkermann, W., Panday, A.K., Lawrence, M.G.: An
900 overview on the airborne measurement in Nepal, part 1: vertical profile of aerosol size-
901 number, spectral absorption and meteorology. Atmos. Chem. Phys. Discuss.
902 https://doi.org/10.5194/acp-2018-95, 2018.
903 Srivastava, R.: Trends in aerosol optical properties over South Asia, Int. J. Climatol., 37, 1, 371-
904 380, DOI: 10.1002/joc.4710, 2016.
905 Storelvmo, T. and Herger, N.: Cirrus cloud susceptibility to the injection of ice nuclei in the upper
906 troposphere. J. Geophys. Res. 119, doi:10.1002/2013JD020816, 2014.
907 Tegen, I. and Lacis, A. A.: Modelling of particle size distribution and its influence on the radiative
908 properties of mineral dust aerosol, J. Geophys. Res.,101, 19,237–19,244 1996.

909 Vadrevu, K.P., Ellicott, E., Badarinath, K.V.S., Vermote, E.: MODIS derived fire characteristics
910 and aerosol optical depth variations during the agricultural residue burning season, north
911 India, Env. Pollution, 159, 1560-1569, 2011.
912 Vaishya, A., Babu, S.S., Jayachandran, V., Gogoi, M.M., Lakshmi, N.B., Moorthy, K.K. and
913 Satheesh, S.K.: Large contrast in the vertical distribution of aerosol optical properties and
914 radiative effects across the Indo-Gangetic Plain during the SWAAMI–RAWEX campaign.
915 Atmos. Chem. Phys., 18, 17669–17685, 2018.
916 Venkataraman, C., Habib, G., Kadamba, D., Shrivastava, M., Leon, J.F., Crouzille, B., Boucher,
917 O. and Streets, D.G.: Emissions from open biomass burning in India: Integrating the
918 inventory approach with high-resolution Moderate Resolution Imaging Spectroradiometer
919 (MODIS) active-fire and land cover data, Global Biogeochem. Cycles, 20, GB2013,
920 doi:10.1029/2005GB002547, 2006.
921 Weingartner, E., Saathoff, H., Schnaiter, M., Streit, N., Bitnar, B. and Baltensperger, U.:
922 Absorption of light by soot particles: Determination of the absorption coefficient by means
923 of aethalometers. J. Aerosol Sci. 34, 1445– 1463, 2003.
924 Yorks, J. E.: An overview of the CATS level 1 processing algorithms and data products,Geophys.
925 Res. Lett., 43, 4632–4639, doi:10.1002/2016GL068006, 2016.
926 Yorks, J. E.: The Airborne Cloud–Aerosol Transport System: Overview and Description of the
927 Instrument and Retrieval Algorithms, J. Atmos. Oceanic Tech., 31, 2482-2497, doi:
928 10.1175/JTECH-D-14-00044.1, 2014.
929 Banerjee, P., Satheesh, S.K., Moorthy, K.K., Nanjundiah, R.S., Nair, V.S.: Long-range transport of
930 mineral dust to the Northeast Indian Ocean: regional versus remote sources and the
931 implications, J. Climate, 32, 1525-1549, doi: 10.1175/JCLI-D-18-0403.1, 2019.
932 GAINS, Greenhouse Gas and Air Pollution Interactions and Synergies - South Asia Program.
933 International Institute of Applied Systems Analysis, Laxenburg, Austria, 2010.
934 Guttikunda, S.K. and Jawahar, P.: Atmospheric emissions and pollution from the coal-fired
935 thermal power plants in India, Atmos. Env. 92, 449-460
936 http://dx.doi.org/10.1016/j.atmosenv.2014.04.057, 2014.
937 Hopkins, R. J., Tivanski, A.V., Marten, B.D., and Gilles, M. K., Chemical bonding and structure of
938 black carbon reference materials and individual carbonaceous atmospheric aerosols, J.
939 Aerosol Sci. 38, 573–591, 2007.

Moorthy, K. K., Babu, S.S., Sunilkumar, S.V., Gupta, P.K., and Gera, B.S.: Altitude profiles of aerosol BC, derived from aircraft measurements over an inland urban location in India, Geophys. Res. Lett. 31, L22103, doi:10.1029/2004GL021336, 2004.

Ricchiazzi, P., Yang, S., Gautier, C., and Sowle, D.: SBDART: A research and teaching software tool for plane-parallel radiative transfer in the Earth's atmosphere, B. Am. Meteor. Soc., 79, 2101–2114, 1998.

Sahu, S.K., Ohara. T., and Beig, G.: The role of coal technology in redefining India's climate change agents and other pollutants Environ. Res. Lett. 12, 105006, https://doi.org/10.1088/1748-9326/aa814a, 2017.

Drinovec, L., Mocnik, G., Zotter, P., Prévôt, A.S.H., Ruckstuhl, C., Coz, E., Rupakheti, M., Sciare, J., Müller, T., Wiedensohler, A., Hansen, A.D.A.: The "dual-spot" Aethalometer: an improved measurement of aerosol black carbon with real-time loading compensation, Atmos. Measurement Tech., 8, 1965-1979, 2015.

Tiwari, M.K., Bajpai, S., Dewangan. U.K., Environmental Issues in Thermal Power Plants – Review in Chhattisgarh Context, J. Mater. Environ. Sci. 10(11), 1123-1134, 2019.

Vaishya, A., Singh, P., Rastogi, S., and Babu, S. S.: Aerosol black carbon quantification in the central Indo-Gangetic Plain: Seasonal heterogeneity and source apportionment, Atmos. Res., 185, 13–21, https://doi.org/10.1016/j.atmosres.2016.10.001, 2017.

Venkataraman., C., Brauer, M., Tibrewal, K., Sadavarte, P., Ma, Q., Cohen, A., Chaliyakunne, S., Frostad, J., Klimont, Z., Martin, R.V., Millet, D.B., Philip, S., Walker, K., and Wang, S.: Source influence on emission pathways and ambient PM2:5 pollution over India (2015–2050), Atmos. Chem. Phys., 18, 8017–8039, https://doi.org/10.5194/acp-18-8017-2018, 2018

Vipradas, M., Babu, Y.D., Garud, S., and Kumar, A., Preparation of road map for mainstreaming wind energy in India, TERI project report No. 2002RT66, The Energy and Resources Institute, 2014.

*****